

SNEAKING UP ON THE CRIEGEE INTERMEDIATE FROM BELOW: PREDICTED PHOTOELECTRON SPECTRUM OF THE CH_2OO^- ANION AND W3-F12 ELECTRON AFFINITY OF CH_2OO

A. Karton

M. Kettner

D. A. Wild*

*School of Chemistry and Biochemistry
The University of Western Australia
M310, 35 Stirling Hwy, Crawley, Australia 6009
duncan.wild@uwa.edu.au*

High level ab initio calculations were undertaken on the CH_2OO anion and neutral species to predict the electron affinity and anion photoelectron spectrum. The electron affinity of CH_2OO , 0.567 eV, and barrier height for dissociation of CH_2OO^- to O^- and CH_2O , 16.5 kJ mol⁻¹, are obtained by means of the W3-F12 thermochemical protocol. Two major geometric differences between the anion and neutral, being the dihedral angle of the terminal hydrogen atoms with respect to C–O–O plane, and the O–O bond length, are reflected in the predicted spectrum as pronounced vibrational progressions.

* Author to whom correspondence should be addressed.

1 Introduction

Elucidation of the properties and reaction pathways of Criegee intermediates has gained fresh momentum recently. These intermediates, first proposed by Criegee in 1949,¹ are of importance in the ozonolysis and breakdown of unsaturated hydrocarbons, which has been shown to be a major pathway in the troposphere leading to OH radicals and particulate matter.^{2–5} The simplest Criegee intermediate is CH₂OO and has in previous work been named formaldehyde oxide, peroxyethylene, or more generally as a carbonyl oxide.

The reason for the renewed activity can be attributed to a breakthrough by Taatjes and co-workers who developed novel gas-phase synthetic techniques for the Criegee intermediates. They first used the chlorine atom initiated reaction with DMSO, followed by photolysis to form CH₂OO,⁶ and shortly after a second route was developed whereby they photolysed CH₂I₂ in the presence of O₂.⁷ In this second study, the authors determined rates of reaction between the Criegee intermediate and atmospherically important species NO, NO₂, SO₂, and H₂O. The group has recently extended their initial study to the next largest Criegee intermediate, namely CH₃CHOO.⁸

Since the breakthrough of this new synthetic approach there has been a burst of activity to characterise the Criegee intermediate by gas-phase IR spectroscopy in the 800 cm⁻¹ to 1500 cm⁻¹ region and determination of the UV absorption cross section and photochemistry.^{9,10} The infrared spectrum was interpreted with the aid of ab initio calculations where three other possible structures for CH₂O₂ were computed, dioxirane, methylenebis(oxy) (also known as dioxymethane), and formic acid, and compared with the experimental spectrum.

Clearly the best match between experiment and theory was with the Criegee intermediate, thereby providing definitive proof of its synthesis. Lester and co-workers reported the UV absorption of the CH₂OO biradical in the 320 nm to 350 nm region, assigned to the B ← X transition,¹⁰ where the excited state (B) is purely repulsive along the O–O coordinate. Results from this work are extremely useful, as they identified the signature of the Criegee intermediate that can be applied in future laboratory or field studies.

The Criegee intermediates have received quite a deal of theoretical attention over the years, with the state of play well represented in References [11], [12] and [13] and references cited therein. Fang et al. studied the potential energy surface of the reaction of CH₂ and O₂ on the singlet and triplet surfaces using CASSCF-type S calculations.¹¹ Nguyen et al.¹² obtained the heat of formation and ionisation energy of the Criegee intermediate at the CCSD(T)/CBS level using W1 theory.¹⁴ It is worthwhile noting that quite recently, Dyke and co-workers used TDDFT, EOM-CCSD, and CASSCF methods to investigate the first few excited electronic states of the simplest CH₂OO intermediate.¹⁵ They also predicted the form of the photoelectron spectrum, i.e. cation ← neutral transitions.

In this contribution, evidence for the stability of the CH₂OO[−] anion from high level W3-F12 calculations is provided. The anion is stable with respect to both autodetachment to the CH₂OO neutral and unimolecular dissociation to CH₂O (formaldehyde) and O[−] products. We believe that it will be possible to characterise the neutral CH₂OO, and possibly larger, Criegee intermediates through anion photoelectron spectroscopy; a valuable method for mapping out the vibrational and electronic states of neutral species. These experiments are appealing as mass spectrometry can be used to isolate the target complex out of an ion population prior to spectroscopic interrogation. There has been

a large volume of work produced in this area from the groups of Lineberger, Neumark, Bowen, Wang, and Kaya, and Johnson with some representative examples provided in references [16–21]. Our laboratory has also recently made contributions in this area.^{22–24}

To the best of the authors' knowledge, there have been no previous computational or experimental investigations of the CH_2OO^- anion. A computational study by Roos and co-workers deals with the dioxirane, dioxymethane, and the dioxymethane anion,²⁵ however the dioxymethane species have both oxygen atoms bound to carbon and not to each other, while for dioxirane there is an O–O bond. There has been experimental work undertaken on very similar species, namely the alkyl peroxides CH_3OO^- and $\text{CH}_3\text{CH}_2\text{OO}^-$. Blanksby et al. produced negative ion photoelectron spectra and determined the adiabatic electron affinities of CH_3OO and $\text{CH}_3\text{CH}_2\text{OO}$ to be 1.161(5) eV and 1.154(4) eV respectively.²⁶ The spectrum of the CH_3OO^- anion showed resolved vibrational progressions in the O–O stretching and $\text{H}_3\text{C}–\text{O}–\text{O}$ bending modes. The spectrum of the $\text{CH}_3\text{CH}_2\text{OO}^-$ also showed well resolved vibrational progressions. Assignment of one progression to the O–O stretch was clear, while a second progression was assigned to a bending mode; however, it was unclear whether it was the C–C–O or C–O–O mode as these modes are predicted to lie very close in frequency. With regard to the alkyl peroxy systems it would be remiss not to make reference to the work undertaken by Xu et al.²⁷ They performed an extensive computational study on the R–OO and R– OO^- anion species with R = CH_3 , C_2H_5 , $n\text{-C}_3\text{H}_7$, $n\text{-C}_4\text{H}_9$, $n\text{-C}_5\text{H}_{11}$, *i*- C_3H_7 , and *t*- C_4H_9 . They predicted the structures, vibrational frequencies, and electron affinities of the neutral species using seven different density functional or hybrid density functional methods.

In the present Letter we obtain the heat of formation and electron affinity of the Criegee intermediate using the recently developed W3-F12 theory.²⁸ W3-F12 represents a layered extrapolation to the relativistic, all-electron CCSDT(Q)/CBS energy (complete basis set limit coupled cluster with singles, doubles, triples, and quasiperturbative quadruple excitations) and shows excellent performance for systems containing first-row elements (and H). Specifically, over the 97 first-row systems in the W4-11 dataset,²⁹ W3-F12 attains a root mean square deviation (RMSD) of only 0.88 kJ mol⁻¹ against all-electron, relativistic reference atomisation energies obtained close to the full configuration interaction (FCI) infinite basis set limit. In addition to the heats of formation and electron affinity of the CH_2OO species, we obtain the barrier height and energy for the $\text{CH}_2\text{OO}^- \rightarrow \text{CH}_2\text{O} + \text{O}^-$ reaction using W3-F12 theory.

2 Computational Methods

The geometries and harmonic frequencies of the anion and neutral CH_2OO species were obtained at the CCSD(T)/A'VQZ level of theory (where A'VnZ indicates the combination of Dunning's aug-cc-pVnZ basis set on carbon and oxygen and the standard cc-pVnZ basis set on hydrogen).^{30,31} The geometry and harmonic frequencies for the transition structure of the $\text{CH}_2\text{OO}^- \rightarrow \text{CH}_2\text{O} + \text{O}^-$ reaction are obtained at the CCSD(T)/A'VTZ level of theory. The optimized geometries for all the species considered in the present work are given as Cartesian coordinate form in Table S1 of the supporting information. All the high-level ab initio calculations were performed using the MOLPRO program suite,³² while all the density functional theory (DFT) calculations were carried out with the GAUSSIAN 09 program suite.³³

The total atomisation energies at the bottom of the well (TAE_e) of the CH_2OO and CH_2OO^- species are obtained by means of the W3-F12 procedure.²⁸ W3-F12 theory combines F12 methods^{34,35} with extrapolation techniques in order to reproduce the CCSDT(Q) basis set limit energy. The CCSD(T)/CBS energy is obtained from the W2-F12 theory and the post-CCSD(T) contributions are obtained from W3.2 theory.³⁶ In brief, the Hartree–Fock component is calculated with the VQZ-F12 basis set (VnZ -F12 denotes the cc-pVnZ-F12 basis sets of Peterson et al. which were developed for explicitly correlated calculations).³⁷ Note that the complementary auxiliary basis (CABS) singles correction is included in the SCF energy.^{38–40} The valence CCSD-F12 correlation energy is extrapolated from the VTZ-F12 and VQZ-F12 basis sets, using the $E(L) = E_\infty + A/L^\alpha$ two-point extrapolation formula, with $\alpha = 3.67$. In all of the explicitly-correlated coupled cluster calculations the diagonal, fixed-amplitude 3C(FIX) ansatz^{38,41,42} and the CCSD-F12b approximation^{39,43} are employed. The quasiperturbative triples, (T), corrections are obtained from standard CCSD(T) calculations (i.e., without inclusion of F12 terms) and scaled by the factor $f = 0.987 \cdot E^{\text{MP2}-\text{F12}}/E^{\text{MP2}}$. This approach has been shown to accelerate the basis set convergence.^{28,43} The higher-order connected triples, T_3 -(T), valence correlation contribution is extrapolated from the cc-pVDZ and cc-pVTZ basis sets using the above two-point extrapolation formula with $\alpha = 3$, and the parenthetical connected quadruples contribution (CCSDT(Q)–CCSDT) is calculated with the cc-pVDZ basis set.³⁶ The CCSD inner-shell contribution is calculated with the core-valence weighted correlation-consistent A'PWCVTZ basis set of Peterson and Dunning,⁴⁴ whilst the (T) inner-shell contribution is calculated with the PWCVTZ(no f) basis set (where A'PWCVTZ indicates the combination of the cc-pVTZ basis set on hydrogen and the aug-cc-pwCVTZ basis set on carbon, and PWCVTZ(no f) indicates the cc-pwCVTZ basis set without the f functions).²⁸ The scalar relativistic contribution (in the second-order Douglas–Kroll–Hess approximation^{45,46}) is obtained as the difference between non-relativistic CCSD(T)/A'VDZ and relativistic CCSD(T)/A'VDZ-DK calculations (where A'VDZ-DK indicates the combination of the cc-pVDZ-DK basis set on H and aug-cc-pVDZ-DK basis set on C and O).⁴⁷ The atomic spin-orbit coupling terms are taken from the experimental fine structure, and the diagonal Born–Oppenheimer corrections (DBOC) are calculated at the HF/A'VTZ level of theory. The zero-point vibrational energies (ZPVEs) are derived from the harmonic frequencies (calculated at the CCSD(T)/A'VQZ level of theory for the CH_2OO and CH_2OO^- species, and the CCSD(T)/A'VTZ level of theory for the $\text{CH}_2\text{O}\cdots\text{O}^-$ transition structure).

The total atomisation energies at 0 K (TAE_0) are converted to heats of formation at 298 K using the Active Thermochemical Tables (ATcT)^{48–50} atomic heats of formation at 0 K (H 216.034(1) kJ mol⁻¹, C 711.38(6) kJ mol⁻¹, and O 246.844(2) kJ mol⁻¹), and the CODATA⁵¹ enthalpy functions, $H_{298} - H_0$, for the elemental reference states ($\text{H}_2(\text{g}) = 8.468(1)$ kJ mol⁻¹ and C(*cr,graphite*) = 1.050(20) kJ mol⁻¹), while the enthalpy functions for the CH_2OO and CH_2OO^- species are obtained within the ridged rotor harmonic oscillator (RRHO) approximation from B3LYP/A'VTZ geometries and harmonic frequencies.^{52–54} Anion photoelectron spectra were simulated by determining the Franck–Condon Factors (FCFs) linking the anion and neutral CH_2OO species vibrational states. FCFs were calculated using the ezSpectrum 3.0 program which is made freely available by Mozhayskiy and Krylov.⁵⁵ The program produces FCFs in either the parallel mode approximation as products of one-dimensional harmonic wavefunctions, or by undertaking Duschinsky rotations of the normal modes between states. Input to the code consists of the output from the ab initio calculations, being geometries, vibrational

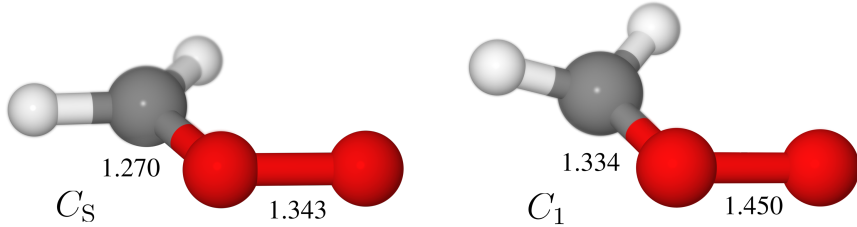
frequencies, and vibrational normal mode vectors. The predicted stick spectra were convoluted with a Gaussian response function of width 0.002 eV to simulate an experimental spectrum.

3 Results & Discussion

3.1 Geometries and vibrational frequencies

The geometry of the neutral Criegee intermediate is well known from previous high level calculations (see Reference [12] and References cited therein). It has been shown that the C–O and O–O bond lengths are sensitive to the level of theory used is, and it is noted that the values predicted from CCSD(T)/A'VQZ calculations are in line with those reported in references [11] and [12]. Our full data set is provided in [Table 1](#), and a visual comparison of the two species is provided in [Figure 1](#). We predict values of 1.270 Å and 1.343 Å for the C–O and O–O bond lengths respectively, which is in very good agreement with the CCSD(T)/AVTZ calculations of Nguyen et al. (1.275 Å and 1.375 Å from reference [12]).

Figure 1: The CH_2OO anion and neutral species. Bond lengths are from CCSD(T)/A'VQZ calculations. Full geometric data are presented in [Table 1](#).



The agreement is also very good between our results and those from Fang et al.^[11] CAS-(8,6)+1+2/cc-pVDZ calculations which result in C–O and O–O bond lengths of 1.280 Å and 1.322 Å respectively. Our CCSD(T)/A'VQZ harmonic vibration frequencies are also in good agreement with those reported previously as shown in [Table 1](#).

To the best of our knowledge, the geometry of the analogous Criegee anion CH_2OO^- and the geometrical parameters (bond lengths r , bond angles θ , and torsional angles ϕ) at the CCSD(T)/A'VQZ level of theory are presented here for the first time. In essence, the structure of the anion is similar to the neutral, as can be seen in [Figure 1](#), however features longer C–O and O–O bond lengths. The C–O bond length increases by 0.064 Å, while the O–O bond length increases by 0.107 Å. In addition to these two structural differences, the anion species is no longer of C_s symmetry as the hydrogen atoms have moved out of the plane defined by the C–O–O atoms. As presented in [Table 1](#), the H–C–O–O dihedral angles are -17.9° and -164.8° for the Criegee anion, whereas in the neutral species the values are 0° and 180° .

Table 1: Computed geometric parameters of the CH_2OO anion and neutral species at the CCSD(T) level of theory, with $A'\text{VQZ}$ or $A'\text{VTZ}$ basis sets.

Basis Set	Anion		Anion TS	Neutral
		CCSD(T)/A'VQZ	CCSD(T)/A'VTZ	CCSD(T)/A'VQZ
$r(\text{C}-\text{H})$	[Å]	1.086, 1.090 [†]	1.093, 1.097 [†]	1.080, 1.082 [†]
$r(\text{C}-\text{O})$	[Å]	1.334	1.317	1.270
$r(\text{O}-\text{O})$	[Å]	1.450	1.589	1.343
$\theta(\text{H}-\text{C}-\text{H})$	[°]	121.1	118.2	126.5
$\theta(\text{H}-\text{C}-\text{O})$	[°]	116.4, 113.0 [†]	118.2, 119.2 [†]	118.7, 114.9 [†]
$\theta(\text{C}-\text{O}-\text{O})$	[°]	111.7	100.7	117.9
$\phi(\text{H}-\text{C}-\text{H}-\text{O})$	[°]	-145.2, 144.1 [†]	-155.9, -156.1 [†]	-180.0
$\phi(\text{H}-\text{C}-\text{O}-\text{O})$	[°]	-17.9, -164.8 [†]	57.1, -98.8 [†]	0.0, 180.0 [†]

[†] Where two values are present, the first corresponds to the hydrogen closest to the terminal oxygen.

In order to rationalise the differences in anion and neutral geometries we have performed natural bond orbital (NBO) calculations to determine the population of the bonding, anti-bonding, and lone pair natural orbitals.⁵⁶ These data, in terms of orbital occupancies, are provided in the supplementary information (Table S4). For the anion species increased electron density is predicted in the lone pair orbitals of the carbon, and for the oxygen bound to carbon. The pyramidal nature of the anion complex, compared with the planar neutral, can be rationalised as the population in the carbon lone pair orbital. The NBO calculations also reveal decreased electron density in C–O and O–O bonding orbitals for the anion, leading to the increase in the bond lengths. There is also a marked decrease in the population of the C–O anti-bonding orbital, whereas the O–O anti-bonding orbital occupancy barely changes. This explains the larger change in the O–O bond length compared with the C–O bond length.

The vibrational modes of the neutral species have been ordered according to the usual numbering scheme appropriate for a C_s symmetry molecule (wavenumber descending in a' , and then descending in a'' symmetry). For ease of comparison between the anion and neutral modes, we have adopted the same order for the anion species even though they are all of a symmetry. In any event, the mode description for each mode is provided in the table. We note that the increased O–O bond length in the anion species is reflected in a reduction of the frequency of the O–O stretching mode, ν_6 , from 945 cm^{-1} to 776 cm^{-1} , similarly the C–O bond length increase leads to a reduction in vibrational frequency of modes ν_3 and ν_4 . The CH_2 wagging mode has also decreased in frequency in the anion species.

3.2 W3-F12 heat of formation and electron affinity of the Criegee intermediate

The components of the W3-F12 total atomisation energies for the CH_2OO and CH_2OO^- species are given in Table 3. At the W2-F12 level, the relativistic, all-electron CCSD(T) contributions to TAE_0 add up to $1520.9\text{ kJ mol}^{-1}$ for CH_2OO , and $1581.5\text{ kJ mol}^{-1}$ for CH_2OO^- . The TAE_0 for the Criegee intermediate is higher than the W1 value of Nguyen et al. by 1.8 kJ mol^{-1} .¹² The lion's share of the difference comes from the va-

Table 2: Computed vibrational data of the CH_2OO anion and neutral species at the CCSD(T)/A'VQZ level, and comparison with recent published work.

Method	Anion		Neutral			Mode description
	CCSD(T)	CCSD(T)	CCSD(T)	NEVPT2		
Basis Set	A'VQZ	A'VQZ	AVTZ	AVDZ		
Approx.	Har.	Har.	Har.	Anh.	Har.	
ν_1 [cm ⁻¹]	3185 a	3302 a'	3290 a'	3370 a'	3149 a'	Asymmetric CH stretch
ν_2 [cm ⁻¹]	3048 a	3140 a'	3137 a'	3197 a'	3030 a'	Symmetric CH stretch
ν_3 [cm ⁻¹]	1422 a	1489 a'	1483 a'	1500 a'	1458 a'	CH_2 scissor/CO stretch
ν_4 [cm ⁻¹]	1252 a	1316 a'	1306 a'	1338 a'	1302 a'	CO stretch/ CH_2 scissor
ν_5 [cm ⁻¹]	1164 a	1239 a'	1231 a'	1235 a'	1220 a'	CH_2 rocking
ν_6 [cm ⁻¹]	776 a	945 a'	935 a'	916 a'	892 a'	OO stretch
ν_7 [cm ⁻¹]	466 a	532 a'	529 a'	536 a'	530 a'	COO deformation
$\dagger\nu_8$ [cm ⁻¹]	601 a	876 a''	862 a''	856 a''	853 a''	CH_2 wagging
$\dagger\nu_9$ [cm ⁻¹]	316 a	651 a''	632 a''	620 a''	606 a''	CH_2 twisting
Reference	This work	This work	[12]	[9]	[9]	as in [9]

† The ordering of the modes of the anion has been changed to reflect that of the neutral, for direct comparison.

lence CCSD(T) components which are closer to the basis set limit in W2-F12 theory ([Table S2](#) of the Supporting Information). The remainder of the difference comes mostly from our better geometry and ZPVE and from the DBOC contribution, which is not included in the W1 values.

We now turn our attention to the post-CCSD(T) contributions to the TAE. [Table S3](#) of the Supporting Information provides a number of a priori diagnostics for the importance of nondynamical correlation effects, namely the percentage of the total atomisation energy accounted for by the SCF and (T) triples contributions from W3-F12 theory^{29,36} (as well as the coupled cluster T₁ and D₁ diagnostics).^{57–59} The CH_2OO neutral and anion species considered in the present study exhibit mild-to-moderate non-dynamical correlation effects; 53 % to 55 % of the atomisation energy is accounted for at the SCF level, and 3.8 % to 4.6 % by the (T) triples. The T₁ diagnostics of above 0.02 (namely, 0.034 to 0.045) and D₁ diagnostics of above 0.05 (0.122 to 0.176) also indicate that post-CCSD(T) excitations may have nontrivial contributions. The generally good performance of the CCSD(T)/CBS level of theory in computational thermochemistry can typically be attributed to the large degree of cancellation between higher-order triples contributions, T₃-(T), and post-CCSDT contributions. For systems dominated by dynamical correlation, these contributions are of similar magnitudes, however, the T₃-(T) excitations tend to universally decrease the atomisation energies whereas the post-CCSDT excitations tend to universally increase the atomisation energies. In this regard, we find that for the CH_2OO^- anion there is a significant degree of cancellation between the T₃-(T) contribution (-2.7 kJ mol^{-1}) and the (Q) contribution (4.5 kJ mol^{-1}). Resulting in a post-CCSD(T) contribution of 1.8 kJ mol^{-1} . However, for the Criegee intermediate there is significantly poorer cancellation between the T₃-(T) (-3.4 kJ mol^{-1}) and (Q) contributions (9.8 kJ mol^{-1}). Therefore, the post-CCSD(T) contributions increase the atomisation energy of CH_2OO by as much as 6.4 kJ mol^{-1} . We note that the inclusion of higher-order quadruple contributions, T₄-(Q), is likely to reduce the magnitude of the connected quadruple excitations, and therefore our CCSDT(Q)/CBS values

should be regarded as upper limits of the TAEs.

Table 3: Component breakdown of the W3-F12 total atomisation energies and heats of formation of the CH_2OO neutral and anion species, electron affinity of CH_2OO , and barrier height for the $\text{CH}_2\text{OO}^- \rightarrow \text{CH}_2\text{O} + \text{O}^-$ reaction (in kJ mol^{-1}).

	CH_2OO	CH_2OO^-	E_{EA}^\dagger	E_{BH}^*
SCF	873.4	903.1	29.7	34.0
CCSD	652.0	685.8	33.7	-4.6
(T)	74.4	62.9	-11.5	-5.8
$\text{T}_3-(\text{T})$	-3.4	-2.7	0.8	-1.9
(Q)	9.8	4.5	-5.3	-1.3
Inner-Shell	5.5	5.2	-0.3	0.5
Scalar Relativistic	-1.9	-2.2	-0.3	-0.2
Spin-Orbit	-2.2	-2.2	0.0	0.0
DBOC	0.3	0.1	-0.1	0.1
TAE _e	1608.0	1654.6	46.6	20.7
ZPVE	80.7	71.3	-9.4	4.3
TAE ₀	1527.3	1583.3	56.1	16.4
$\Delta H_{\text{f},0}$	109.9	53.8	56.1	16.4
$\Delta H_{\text{f},298}$	102.8	48.1	54.7	16.5

† Energy for the $\text{CH}_2\text{OO}^- \rightarrow \text{CH}_2\text{OO} + \text{e}^-$ reaction.

* Barrier height for the $\text{CH}_2\text{OO}^- \rightarrow \text{CH}_2\text{O} + \text{O}^-$ reaction.

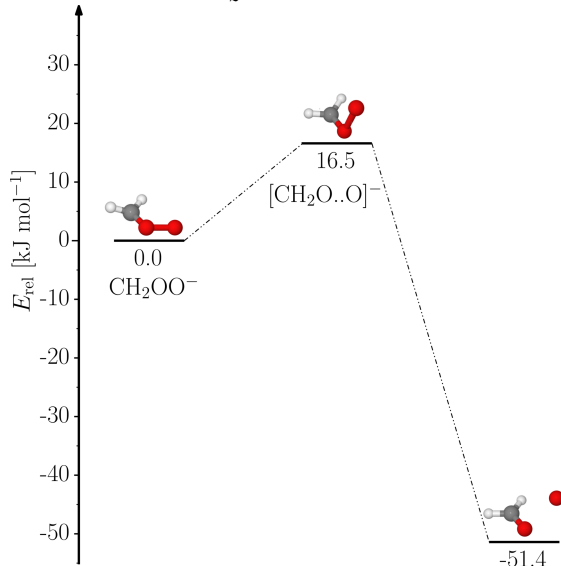
Overall, our best relativistic, all-electron CCSDT(Q)/CBS atomisation energies (Table 3) are $1527.3 \text{ kJ mol}^{-1}$ (CH_2OO) and $1583.3 \text{ kJ mol}^{-1}$ (CH_2OO^-). These correspond to heats of formation at 0 K of $109.9 \text{ kJ mol}^{-1}$ (CH_2OO) and 53.8 kJ mol^{-1} (CH_2OO^-), and heats of formation at 298 K of $102.8 \text{ kJ mol}^{-1}$ (CH_2OO) and 48.1 kJ mol^{-1} (CH_2OO^-). In accordance with the large post-CCSD(T) contributions for the Criegee intermediate our W3-F12 heats of formation are lower than the W1 values of Nguyen et al.¹² ($\Delta H_{\text{f},0} = 113.0 \text{ kJ mol}^{-1}$ and $\Delta H_{\text{f},298} = 105.9 \text{ kJ mol}^{-1}$).

Using the W3-F12 heats of formation for the CH_2OO neutral and anion species electron affinities for the Criegee intermediate of 56.1 kJ mol^{-1} at 0 K and 54.7 kJ mol^{-1} at 298 K were obtained. It is noted that the post-CCSD(T) contributions to the electron affinity add up to as much as 4.5 kJ mol^{-1} .

3.3 Stability of CH_2OO^- with respect to dissociation

In order to determine the stability of the Criegee anion species we modelled the reaction profile for dissociation to the products formaldehyde and oxide. This was achieved by optimising the geometry of the transition state (TS) linking the reactant CH_2OO^- and the products CH_2O and O^- species. The W3-F12 procedure was applied to the TS, anion, and products with the results shown in Figure 2. It is clear that an appreciable barrier to dissociation exists of 16.5 kJ mol^{-1} , and therefore should a synthetic route to the anion be found it is likely that it should survive long enough for interrogation.

Figure 2: Reaction profile illustrating the dissociation channel of the Criegee anion CH_2OO^- to the products $\text{CH}_2\text{O} + \text{O}^-$ calculated at the W3-F12 level.



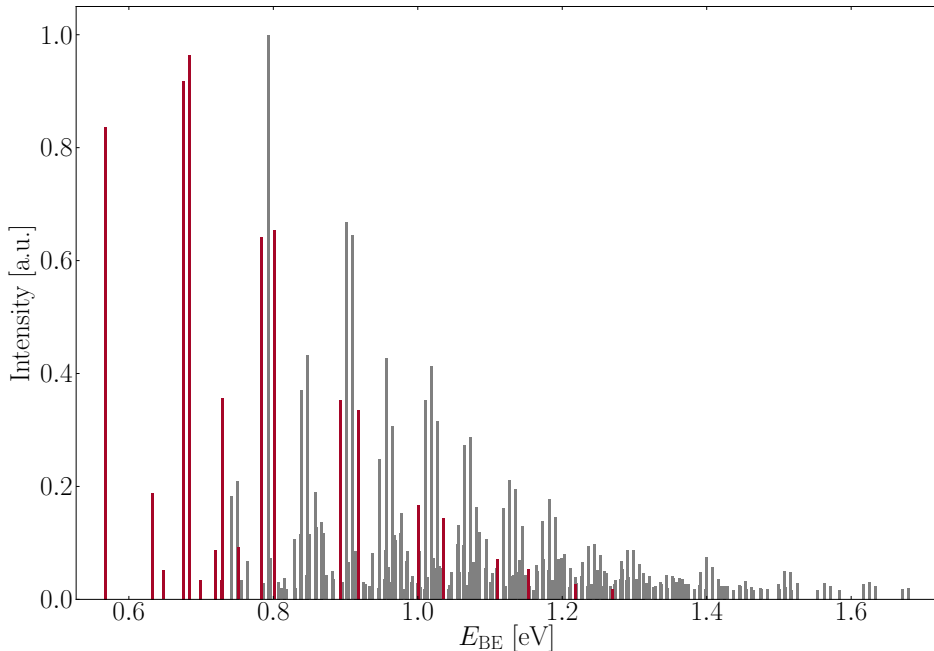
3.4 Predicted anion photoelectron spectrum of CH_2OO^-

Armed with the CCSD(T)/A'VQZ geometries, vibrational frequencies, and normal mode vectors, we are in a position to predict the form of the anion photoelectron spectrum. Therefore the ezSpectrum 3.0 code was employed to simulate the vibronic transitions at a temperature of 10 K, which is appropriate for species entrained in a molecular beam produced via supersonic expansion. Up to 10 quanta were allowed in each excited state vibrational mode (i.e. the modes of the neutral CH_2OO species). In Figure 3, a stick spectrum is presented which is the result of applying the ezSpectrum code with the Duschinsky approach. We also performed simulations using the parallel mode approximation, however, the differences between the forms of the two predicted spectra were insignificant and do not warrant further discussion. The grey part of the spectrum marks the combination bands, whereas the red part represents the pure progressions; together they form the fully predicted spectrum. Data pertaining to this spectrum, including predicted line positions, intensities, Franck-Condon Factors, and assignments, are provided in the supplementary information (Table S5 and Table S6) accompanying this Letter.

The majority of the pure progressions (marked red in Figure 3) are for the modes ν_6 and ν_8 which correspond to the O–O stretching and CH_2 wagging modes respectively. The fact that these two modes display the longest progressions is consistent with the geometry changes observed between the anion and neutral species. Referring to the data in Table 1, the O–O bond length is predicted to decrease by 0.107 Å, while the two hydrogen atoms move into the C–O–O plane, with the pair of H–C–O–O dihedral angles changing from -17.9° and -164.8° to 0.0° and 180.0° . The low panel of Figure 3 includes the possible combination bands, i.e. those with intensity above the cut off threshold of 0.001 au. The major combination bands are again those associate with the O–O and CH_2 wagging modes.

Again, a full list of line positions including assignments is provided in the supplemen-

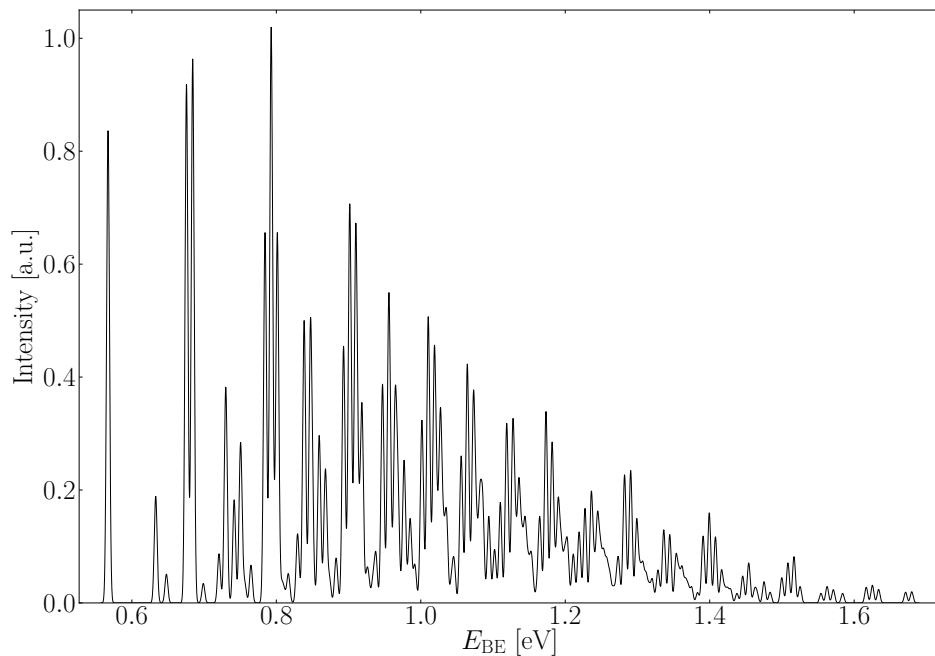
Figure 3: Predicted anion photoelectron stick spectra (red marks the pure progressions).



tary material. To provide a clearer picture of what an experimental spectrum might look like, we convoluted the line spectrum with a Gaussian response function whose full width at half maximum was set to 0.002 eV and the resulting simulated spectrum is shown in Figure 4. We believe that this is appropriate as this resolution is achievable by the state-of-the-art anion photoelectron spectrometers in use today.

As a final note, when considering the mass selected photoelectron spectrum of the CH_2OO^- anion one cannot discount the possibility that a van der Waals complex of the form $\text{O}^- \cdots \text{CH}_2\text{O}$ may also be synthesised in addition to the covalently bound CH_2OO^- anion. This possibility needs to be taken into account, however, fortuitously the ionisation energy of the O^- anion is a great deal larger than for CH_2OO^- , with the most recent determination of the electron affinity of the O neutral being 1.439 157 eV.⁶⁰ The $\text{O}^- \cdots \text{CH}_2\text{O}$ species should be essentially a perturbed O^- anion, due to the weak interaction in a van Der Waals species, and in addition the electron binding energy of the anion generally increases upon formation of a van der Waals complex. Therefore, the Criegee anion can be preferentially targeted by selecting a photodetachment photon energy below 1.4 eV.

Figure 4: Simulated photoelectron spectrum of CH_2OO^- with the stick spectrum shown in Figure 3 convoluted with Gaussian response function ($fwhm = 2 \text{ meV}$).



4 Summary

In summary, we have shown that the CH_2OO^- anion with an analogous structure to the neutral Criegee intermediate exists. The anion is stable with respect to dissociation of the O–O bond, with a barrier of 16.5 kJ mol^{-1} , and the electron is bound by 0.567 eV . The major geometric differences between the anion and neutral are in the increased O–O bond length, and the movement of the terminal hydrogen atoms into the plane formed by the C–O–O atoms. Progressions involving both of these modes are prominent in the predicted photoelectron spectrum.

Acknowledgements

We gratefully acknowledge funding (to A.K.) from the Australian Research Council (Discovery Project Grant: DP110102336) and the generous allocation of computing time from the National Computational Infrastructure (NCI) National Facility.

References

- [1] R. Criegee and G. Wenner. “Die Ozonisierung des 9,10-Oktalins”. In: *Justus Liebigs Annalen der Chemie* 564.1 (1949), pp. 9–15. ISSN: 1099-0690. doi: [10.1002/jlac.19495640103](https://doi.org/10.1002/jlac.19495640103).

- [2] D. Johnson and G. Marston. “The gas-phase ozonolysis of unsaturated volatile organic compounds in the troposphere”. In: *Chemical Society Reviews* 37 (4 2008), pp. 699–716. DOI: [10.1039/B704260B](https://doi.org/10.1039/B704260B).
- [3] A. S. Hasson, K. T. Kuwata, M. C. Arroyo, and E. B. Petersen. “Theoretical studies of the reaction of hydroperoxy radicals (HO_2) with ethyl peroxy ($\text{CH}_3\text{CH}_2\text{O}_2$), acetyl peroxy ($\text{CH}_3\text{C}(\text{O})\text{O}_2$), and acetonyl peroxy ($\text{CH}_3\text{C}(\text{O})\text{CH}_2\text{O}_2$) radicals”. In: *Journal of Photochemistry and Photobiology A: Chemistry* 176.1–3 (2005), pp. 218–230. ISSN: 1010-6030. DOI: <http://dx.doi.org/10.1016/j.jphotochem.2005.08.012>.
- [4] R. Gutbrod, E. Kraka, R. N. Schindler, and D. Cremer. “Kinetic and Theoretical Investigation of the Gas-Phase Ozonolysis of Isoprene: Carbonyl Oxides as an Important Source for OH Radicals in the Atmosphere”. In: *Journal of the American Chemical Society* 119.31 (1997), pp. 7330–7342. DOI: [10.1021/ja970050c](https://doi.org/10.1021/ja970050c).
- [5] R. Gutbrod, R. N. Schindler, E. Kraka, and D. Cremer. “Formation of OH radicals in the gas phase ozonolysis of alkenes: the unexpected role of carbonyl oxides”. In: *Chemical Physics Letters* 252.3–4 (1996), pp. 221–229. ISSN: 0009-2614. DOI: [http://dx.doi.org/10.1016/0009-2614\(96\)00126-1](http://dx.doi.org/10.1016/0009-2614(96)00126-1).
- [6] C. A. Taatjes, G. Meloni, T. M. Selby, A. J. Trevitt, D. L. Osborn, C. J. Percival, and D. E. Shallcross. “Direct Observation of the Gas-Phase Criegee Intermediate (CH_2OO)”. In: *Journal of the American Chemical Society* 130.36 (2008), pp. 11883–11885. DOI: [10.1021/ja804165q](https://doi.org/10.1021/ja804165q).
- [7] O. Welz, J. D. Savee, D. L. Osborn, S. S. Vasu, C. J. Percival, D. E. Shallcross, and C. A. Taatjes. “Direct Kinetic Measurements of Criegee Intermediate (CH_2OO) Formed by Reaction of CH_2I with O_2 ”. In: *Science* 335.6065 (2012), pp. 204–207. DOI: [10.1126/science.1213229](https://doi.org/10.1126/science.1213229).
- [8] C. A. Taatjes, O. Welz, A. J. Eskola, J. D. Savee, A. M. Scheer, D. E. Shallcross, B. Rotavera, E. P. F. Lee, J. M. Dyke, et al. “Direct Measurements of Conformer-Dependent Reactivity of the Criegee Intermediate CH_3CHO ”. In: *Science* 340.6129 (2013), pp. 177–180. DOI: [10.1126/science.1234689](https://doi.org/10.1126/science.1234689).
- [9] Y.-T. Su, Y.-H. Huang, H. A. Witek, and Y.-P. Lee. “Infrared Absorption Spectrum of the Simplest Criegee Intermediate CH_2OO ”. In: *Science* 340.6129 (2013), pp. 174–176. DOI: [10.1126/science.1234369](https://doi.org/10.1126/science.1234369).
- [10] J. M. Beames, F. Liu, L. Lu, and M. I. Lester. “Ultraviolet Spectrum and Photochemistry of the Simplest Criegee Intermediate CH_2OO ”. In: *Journal of the American Chemical Society* 134.49 (2012), pp. 20045–20048. DOI: [10.1021/ja310603j](https://doi.org/10.1021/ja310603j).
- [11] D.-C. Fang and X.-Y. Fu. “CASSCF and CAS+1+2 Studies on the Potential Energy Surface and the Rate Constants for the Reactions between CH_2 and O_2 ”. In: *The Journal of Physical Chemistry A* 106.12 (2002), pp. 2988–2993. DOI: [10.1021/jp014129m](https://doi.org/10.1021/jp014129m).
- [12] M. T. Nguyen, T. L. Nguyen, V. T. Ngan, and H. M. T. Nguyen. “Heats of formation of the Criegee formaldehyde oxide and dioxirane”. In: *Chemical Physics Letters* 448.4–6 (2007), pp. 183–188. ISSN: 0009-2614. DOI: [10.1016/j.cplett.2007.10.033](https://doi.org/10.1016/j.cplett.2007.10.033).
- [13] L. Vereecken and J. S. Francisco. “Theoretical studies of atmospheric reaction mechanisms in the troposphere”. In: *Chemical Society Reviews* 41 (19 2012), pp. 6259–6293. DOI: [10.1039/C2CS35070J](https://doi.org/10.1039/C2CS35070J).
- [14] J. M. L. Martin and G. de Oliveira. “Towards standard methods for benchmark quality ab initio thermochemistry—W1 and W2 theory”. In: *The Journal of Chemical Physics* 111.5 (1999), pp. 1843–1856. DOI: [10.1063/1.479454](https://doi.org/10.1063/1.479454).
- [15] E. P. F. Lee, D. K. W. Mok, D. E. Shallcross, C. J. Percival, D. L. Osborn, C. A. Taatjes, and J. M. Dyke. “Spectroscopy of the Simplest Criegee Intermediate CH_2OO : Simulation of the First Bands in Its Electronic and Photoelectron Spectra”. In: *Chemistry – A European Journal* 18.39 (2012), pp. 12411–12423. ISSN: 1521-3765. DOI: [10.1002/chem.201200848](https://doi.org/10.1002/chem.201200848).
- [16] B. M. Elliott, L. R. McCunn, and M. A. Johnson. “Photoelectron imaging study of vibrationally mediated electron autodetachment in the type I isomer of the water hexamer anion”. In: *Chemical Physics Letters* 467.1–3 (2008), pp. 32–36. ISSN: 0009-2614. DOI: <http://dx.doi.org/10.1016/j.cplett.2008.11.008>.

- [17] R. M. Calvi, D. H. Andrews, and W. C. Lineberger. “Negative ion photoelectron spectroscopy of copper hydrides”. In: *Chemical Physics Letters* 442.1–3 (2007), pp. 12–16. ISSN: 0009-2614. doi: <http://dx.doi.org/10.1016/j.cplett.2007.05.060>.
- [18] A. Kammerath, J. R. R. Verlet, G. B. Griffin, and D. M. Neumark. “Photoelectron spectroscopy of large $(\text{H}_2\text{O})_n^-$ ($n = 50\text{--}200$) clusters at 4.7 eV”. In: *The Journal of Chemical Physics* 125.7, 076101 (2006), p. 076101. doi: <10.1063/1.2217745>.
- [19] J. Jellinek, P. H. Acioli, J. García-Rodeja, W. Zheng, O. C. Thomas, and K. H. Bowen. “ Mn_n^- clusters: Size-induced transition to half metallicity”. In: *Phys. Rev. B* 74 (15 2006), p. 153401. doi: <10.1103/PhysRevB.74.153401>.
- [20] X. Li and L.-S. Wang. “Probing the electronic structure of mono-nitrogen doped aluminum clusters using anion photoelectron spectroscopy”. English. In: *The European Physical Journal D - Atomic, Molecular, Optical and Plasma Physics* 34.1–3 (2005), pp. 9–14. ISSN: 1434-6060. doi: <10.1140/epjd/e2005-00100-3>.
- [21] M. Ohara, K. Miyajima, A. Pramann, A. Nakajima, and K. Kaya. “Geometric and Electronic Structures of Terbium-Silicon Mixed Clusters (TbSi_n ; $6 \leq n \leq 16$)”. In: *The Journal of Physical Chemistry A* 106.15 (2002), pp. 3702–3705. doi: <10.1021/jp012952c>.
- [22] K. Lapere, R. LaMacchia, L. Quak, A. McKinley, and D. Wild. “Anion photoelectron spectroscopy and ab initio calculations of the gas phase chloride-carbon monoxide complex: $\text{Cl}^- - \dots \text{CO}$ ”. In: *Chemical Physics Letters* 504.1–3 (2011), pp. 13–19. ISSN: 0009-2614. doi: <10.1016/j.cplett.2011.01.034>.
- [23] K. M. Lapere, R. J. LaMacchia, L. H. Quak, M. Kettner, S. G. Dale, A. J. McKinley, and D. A. Wild. “The Bromide–Carbon Monoxide Gas Phase Complex: Anion Photoelectron Spectroscopy and Ab Initio Calculations”. In: *Australian Journal of Chemistry* 65 (2012), pp. 457–463. doi: <10.1071/CH12007>.
- [24] K. M. Lapere, R. J. LaMacchia, L. H. Quak, M. Kettner, S. G. Dale, A. J. McKinley, and D. A. Wild. “Anion Photoelectron Spectra and Ab Initio Calculations of the Iodide–Carbon Monoxide Clusters: $\text{I}^- \dots (\text{CO})_n$, $n = 1\text{--}4$ ”. In: *The Journal of Physical Chemistry A* 116.14 (2012), pp. 3577–3584. doi: <10.1021/jp300471x>.
- [25] M. Cantos, M. Merchán, F. Tomás-Vert, and B. O. Roos. “A theoretical study of the geometry and electronic spectra of dioxirane, dioxymethane and its anion”. In: *Chemical Physics Letters* 229.3 (1994), pp. 181–190. doi: [10.1016/0009-2614\(94\)01040-4](10.1016/0009-2614(94)01040-4).
- [26] S. J. Blanksby, T. M. Ramond, G. E. Davico, M. R. Nimlos, S. Kato, V. M. Bierbaum, W. C. Lineberger, G. B. Ellison, and M. Okumura. “Negative-Ion Photoelectron Spectroscopy, Gas-Phase Acidity, and Thermochemistry of the Peroxyl Radicals CH_3OO and $\text{CH}_3\text{CH}_2\text{OO}$ ”. In: *Journal of the American Chemical Society* 123.39 (2001), pp. 9585–9596. doi: <10.1021/ja010942j>.
- [27] W. Xu and G. Lu. “Structures, Electron Affinities, and Harmonic Vibrational Frequencies of the Simplest Alkyl Peroxyl Radicals and Their Anions”. In: *The Journal of Physical Chemistry A* 112.30 (2008), pp. 6999–7014. doi: <10.1021/jp7118923>.
- [28] A. Karton and J. M. L. Martin. “Explicitly correlated Wn theory: W1-F12 and W2-F12”. In: *The Journal of Chemical Physics* 136.12, 124114 (2012), p. 124114. doi: <10.1063/1.3697678>.
- [29] A. Karton, S. Daon, and J. M. Martin. “W4-11: A high-confidence benchmark dataset for computational thermochemistry derived from first-principles {W4} data”. In: *Chemical Physics Letters* 510.4–6 (2011), pp. 165–178. ISSN: 0009-2614. doi: <http://dx.doi.org/10.1016/j.cplett.2011.05.007>.
- [30] T. H. Dunning. “Gaussian basis sets for use in correlated molecular calculations. I. The atoms boron through neon and hydrogen”. In: *The Journal of Chemical Physics* 90.2 (1989), pp. 1007–1023. doi: <10.1063/1.456153>.
- [31] R. A. Kendall, T. H. Dunning, and R. J. Harrison. “Electron affinities of the first-row atoms revisited. Systematic basis sets and wave functions”. In: *The Journal of Chemical Physics* 96.9 (1992), p. 035401. doi: <10.1063/1.462569>.

- [32] H.-J. Werner, P. J. Knowles, G. Knizia, F. R. Manby, M. Schütz, P. Celani, T. Korona, R. Lindh, A. Mitrushenkov, et al. *MOLPRO, version 2012.1, a package of ab initio programs*. see <http://www.molpro.net>. Cardiff, UK, 2012.
- [33] M. J. Frisch, G. W. Trucks, H. B. Schlegel, G. E. Scuseria, M. A. Robb, J. R. Cheeseman, G. Scalmani, V. Barone, B. Mennucci, et al. *Gaussian 09 Revision A.1*. Gaussian Inc. Wallingford CT 2009.
- [34] K. A. Peterson, D. Feller, and D. Dixon. “Chemical accuracy in ab initio thermochemistry and spectroscopy: current strategies and future challenges”. English. In: *Theoretical Chemistry Accounts* 131.1 (2012), pp. 1–20. ISSN: 1432-881X. doi: [10.1007/s00214-011-1079-5](https://doi.org/10.1007/s00214-011-1079-5).
- [35] S. Ten-no and J. Noga. “Explicitly correlated electronic structure theory from R12/F12 ansätze”. In: *Wiley Interdisciplinary Reviews: Computational Molecular Science* 2.1 (2012), pp. 114–125. ISSN: 1759-0884. doi: [10.1002/wcms.68](https://doi.org/10.1002/wcms.68).
- [36] A. Karton, E. Rabinovich, J. M. L. Martin, and B. Ruscic. “W4 theory for computational thermochemistry: In pursuit of confident sub-kJ/mol predictions”. In: *The Journal of Chemical Physics* 125.14, 144108 (2006), p. 144108. doi: [10.1063/1.2348881](https://doi.org/10.1063/1.2348881).
- [37] K. A. Peterson, T. B. Adler, and H.-J. Werner. “Systematically convergent basis sets for explicitly correlated wavefunctions: The atoms H, He, B–Ne, and Al–Ar”. In: *The Journal of Chemical Physics* 128.8, 084102 (2008), p. 084102. doi: [10.1063/1.2831537](https://doi.org/10.1063/1.2831537).
- [38] G. Knizia and H.-J. Werner. “Explicitly correlated RMP2 for high-spin open-shell reference states”. In: *The Journal of Chemical Physics* 128.15, 154103 (2008), p. 154103. doi: [10.1063/1.2889388](https://doi.org/10.1063/1.2889388).
- [39] T. B. Adler, G. Knizia, and H.-J. Werner. “A simple and efficient CCSD(T)-F12 approximation”. In: *The Journal of Chemical Physics* 127.22, 221106 (2007), p. 221106. doi: [10.1063/1.2817618](https://doi.org/10.1063/1.2817618).
- [40] J. Noga, S. Kedzuch, and J. Simunek. “Second order explicitly correlated R12 theory revisited: A second quantization framework for treatment of the operators’ partitionings”. In: *The Journal of Chemical Physics* 127.3, 034106 (2007), p. 034106. doi: [10.1063/1.2751163](https://doi.org/10.1063/1.2751163).
- [41] S. Ten-no. “Initiation of explicitly correlated Slater-type geminal theory”. In: *Chemical Physics Letters* 398.1–3 (2004), pp. 56–61. ISSN: 0009-2614. doi: <http://dx.doi.org/10.1016/j.cplett.2004.09.041>.
- [42] H.-J. Werner, G. Knizia, and F. R. Manby. “Explicitly correlated coupled cluster methods with pair-specific geminals”. In: *Molecular Physics* 109.3 (2011), pp. 407–417. doi: [10.1080/00268976.2010.526641](https://doi.org/10.1080/00268976.2010.526641).
- [43] G. Knizia, T. B. Adler, and H.-J. Werner. “Simplified CCSD(T)-F12 methods: Theory and benchmarks”. In: *The Journal of Chemical Physics* 130.5, 054104 (2009), p. 054104. doi: [10.1063/1.3054300](https://doi.org/10.1063/1.3054300).
- [44] K. A. Peterson and J. Thom H. Dunning. “Accurate correlation consistent basis sets for molecular core–valence correlation effects: The second row atoms Al–Ar, and the first row atoms B–Ne revisited”. In: *The Journal of Chemical Physics* 117.23 (2002), pp. 10548–10560. doi: [10.1063/1.1520138](https://doi.org/10.1063/1.1520138).
- [45] M. Douglas and N. M. Kroll. “Quantum electrodynamical corrections to the fine structure of helium”. In: *Annals of Physics* 82.1 (1974), pp. 89–155. ISSN: 0003-4916. doi: [http://dx.doi.org/10.1016/0003-4916\(74\)90333-9](http://dx.doi.org/10.1016/0003-4916(74)90333-9).
- [46] B. A. Hess. “Relativistic electronic-structure calculations employing a two-component no-pair formalism with external-field projection operators”. In: *Phys. Rev. A* 33 (6 1986), pp. 3742–3748. doi: [10.1103/PhysRevA.33.3742](https://doi.org/10.1103/PhysRevA.33.3742).
- [47] W. A de Jong, R. J. Harrison, and D. A. Dixon. “Parallel Douglas–Kroll energy and gradients in NWChem: Estimating scalar relativistic effects using Douglas–Kroll contracted basis sets”. In: *The Journal of Chemical Physics* 114.1 (2001), pp. 48–53. doi: [10.1063/1.1329891](https://doi.org/10.1063/1.1329891).
- [48] B. Ruscic, R. E. Pinzon, M. L. Morton, G. von Laszewski, S. J. Bittner, S. G. Nijssure, K. A. Amin, M. Minkoff, and A. F. Wagner. “Introduction to Active Thermochemical Tables: Several ‘Key’ Enthalpies of Formation Revisited†”. In: *The Journal of Physical Chemistry A* 108.45 (2004), pp. 9979–9997. doi: [10.1021/jp047912y](https://doi.org/10.1021/jp047912y).

- [49] W. R. Stevens, B. Ruscic, and T. Baer. “Heats of Formation of C₆H₅·, C₆H₅+, and C₆H₅NO by Threshold Photoelectron Photoion Coincidence and Active Thermochemical Tables Analysis”. In: *The Journal of Physical Chemistry A* 114.50 (2010), pp. 13134–13145. doi: [10.1021/jp107561s](https://doi.org/10.1021/jp107561s).
- [50] B. Ruscic, R. E. Pinzon, M. L. Morton, N. K. Srinivasan, M.-C. Su, J. W. Sutherland, and J. V. Michael. “Active Thermochemical Tables: Accurate Enthalpy of Formation of Hydroperoxyl Radical, HO₂”. In: *The Journal of Physical Chemistry A* 110.21 (2006), pp. 6592–6601. doi: [10.1021/jp056311j](https://doi.org/10.1021/jp056311j).
- [51] J. D. Cox, D. D. Wagman, and V. A. Medvedev. *CODATA Key Values for Thermodynamics*. see <http://www.codata.org>. New York, 1989.
- [52] A. D. Becke. “Density-functional thermochemistry. III. The role of exact exchange”. In: *The Journal of Chemical Physics* 98.7 (1993), pp. 5648–5652. doi: [10.1063/1.464913](https://doi.org/10.1063/1.464913).
- [53] P. J. Stephens, F. J. Devlin, C. F. Chabalowski, and M. J. Frisch. “Ab Initio Calculation of Vibrational Absorption and Circular Dichroism Spectra Using Density Functional Force Fields”. In: *The Journal of Physical Chemistry* 98.45 (1994), pp. 11623–11627. doi: [10.1021/j100096a001](https://doi.org/10.1021/j100096a001).
- [54] C. Lee, W. Yang, and R. G. Parr. “Development of the Colle-Salvetti correlation-energy formula into a functional of the electron density”. In: *Phys. Rev. B* 37 (2 1988), pp. 785–789. doi: [10.1103/PhysRevB.37.785](https://doi.org/10.1103/PhysRevB.37.785).
- [55] V. Mozhayskiy and A. Krylov. *ezSpectrum*. see <http://iopenshell.usc.edu/downloads>.
- [56] E. D. G. J, K. Badenhoop, A. E. Reed, J. E. Carpenter, J. A. Bohmann, C. M. Morales, C. R. Landis, and F. Weinhold. *NBO 6.0*. Theoretical Chemistry Institute, University of Wisconsin, Madison (2013).
- [57] T. J. Lee. “Comparison of the *T*₁ and *D*₁ diagnostics for electronic structure theory: a new definition for the open-shell *D*₁ diagnostic”. In: *Chemical Physics Letters* 372.3–4 (2003), pp. 362–367. doi: [http://dx.doi.org/10.1016/S0009-2614\(03\)00435-4](http://dx.doi.org/10.1016/S0009-2614(03)00435-4).
- [58] M. L. Leininger, I. M. Nielsen, T. Crawford, and C. L. Janssen. “A new diagnostic for open-shell coupled-cluster theory”. In: *Chemical Physics Letters* 328.4–6 (2000), pp. 431–436. doi: [http://dx.doi.org/10.1016/S0009-2614\(00\)00966-0](http://dx.doi.org/10.1016/S0009-2614(00)00966-0).
- [59] T. J. Lee, J. E. Rice, G. E. Scuseria, and H. F. Schaefer III. “Theoretical investigations of molecules composed only of fluorine, oxygen and nitrogen: determination of the equilibrium structures of FOOF, (NO)₂ and FNNF and the transition state structure for FNNF cis-trans isomerization”. English. In: *Theoretica chimica acta* 75.2 (1989), pp. 81–98. ISSN: 0040-5744. doi: [10.1007/BF00527711](https://doi.org/10.1007/BF00527711).
- [60] A. Joiner, R. H. Mohr, and J. N. Yukich. “High-resolution photodetachment spectroscopy from the lowest threshold of O⁻”. In: *Physical Review A* 83.3 (2011), pp. 6796–6806. doi: [10.1103/PhysRevA.83.035401](https://doi.org/10.1103/PhysRevA.83.035401).

Supporting Information

Table S1: CCSD(*T*) Optimised Geometries (Cartesian Coordinates in Å).

CH ₂ OO optimised at CCSD(T)/A'VQZ			
	x	y	z
C	1.074 790 954 2	-0.206 575 928 2	0.000 000 000 0
H	1.979 677 245 9	0.382 186 173 1	0.000 000 000 0
O	-0.001 515 793 3	0.468 205 695 8	0.000 000 000 0
O	-1.165 017 699 7	-0.202 933 042 7	0.000 000 000 0
H	1.010 308 292 8	-1.287 087 898 1	0.000 000 000 0
CH ₂ OO ⁻ optimised at CCSD(T)/A'VQZ			
	x	y	z
C	1.101 533 191 7	-0.229 149 572 5	-0.063 060 084 4
H	2.016 025 265 1	0.292 700 141 6	0.217 757 295 6
O	0.015 166 596 1	0.540 425 223 7	0.018 566 420 1
O	-1.202 320 126 9	-0.247 146 831 5	-0.011 696 225 5
H	0.965 446 073 7	-1.282 404 961 2	0.162 484 594 0
CH ₂ OO optimised at CCSD(T)/A'VTZ			
	x	y	z
C	1.076 818 676 4	-0.207 035 849 0	0.000 000 000 0
H	1.982 960 111 8	0.381 979 796 1	0.000 000 000 0
O	-0.002 618 673 2	0.471 610 046 4	0.000 000 000 0
O	-1.171 291 535 4	-0.204 129 142 2	0.000 000 000 0
H	1.012 374 420 3	-1.288 629 851 3	0.000 000 000 0
CH ₂ OO ⁻ optimised at CCSD(T)/A'VTZ			
	x	y	z
C	1.103 699 235 3	-0.229 595 995 0	-0.067 263 693 4
H	2.018 367 937 7	0.291 711 456 4	0.219 638 441 0
O	0.014 965 709 8	0.544 038 620 6	0.019 280 622 0
O	-1.208 803 653 1	-0.248 724 066 3	-0.011 729 182 8
H	0.967 621 770 2	-1.283 006 015 7	0.164 125 813 2
[CH ₂ O ··· O] ⁻ optimised at CCSD(T)/A'VTZ			
	x	y	z
C	1.074 380 845 2	-0.232 703 156 6	-0.027 400 208 0
H	1.060 086 786 0	-1.085 529 818 0	-0.710 223 499 9
O	0.101 821 301 9	0.650 944 598 5	-0.116 593 427 5
O	-1.165 421 797 0	-0.282 942 983 5	0.101 191 128 7
H	1.618 109 863 8	-0.335 489 640 4	0.919 673 006 7

Table S2: Comparison between W2-F12 (*this work*) and W1^a CCSD(T)/CBS total atomisation energies for the Criegee intermediate (in kJ mol⁻¹).

	CCSD(T)/CBS	CV+SR	SO	ZPVE	TAE(0)
W2-F12	1599.9	3.6	-2.2	80.7	1520.9
W1	1598.7	3.7	-2.2	80.1	1519.1

a Taken from M.T. Nguyen, T.L. Nguyen, V.T. Ngan, H.M.T. Nguyen, Chem. Phys. Lett., 448 (2007) 183.

Table S3: Diagnostics for importance of nondynamical correlation.

	CH ₂ OO	CH ₂ OO ⁻	[CH ₂ O ··· O] ⁻
TAE[SCF] ^a [%]	54.4	54.6	53.2
TAE _e [(T)] ^b [%]	4.6	3.8	4.2
T1 ^c	0.044	0.034	0.045
D1 ^c	0.176	0.122	0.130

a Percentages of the total atomisation energy accounted by the SCF component relative to nonrelativistic, clamped-nuclei, valence CCSDT(Q) values from W3-F12 theory.

b Percentages of the total atomisation energy accounted by the (T) component relative to nonrelativistic, clamped-nuclei, valence CCSDT(Q) values from W3-F12 theory.

c From a CCSD(T)/A'VTZ calculation.

Table S4: Orbital occupancies from NBO 6.0 calculations for anion and neutral CH₂OO.

	CH ₂ OO	CH ₂ OO ⁻
C–O bonding	3.9959	2.9960
O–O bonding	1.9913	1.9873
C–O anti-bonding	0.1316	0.0180
O–O anti-bonding	0.0085	0.0088
C lone pair	0.0000	0.9933
O lone pair	1.9780	2.9706
O lone pair (terminal)	5.8510	5.9699
C–H bonding	1.9891/1.9955	1.9899/1.9956
C–H anti-bonding	0.0115/0.0153	0.0127/0.0166

Table S5: ezSpectrum 3.0 simulations from CCSD(T)/A'VQZ geometries, harmonic frequencies and normal mode vectors. Data pertain to application of the Duschinsky formalism. Simulation temperature of 10 K, intensity threshold of 1.0 × 10⁻³ au, maximum number of quanta in excited state $v = 10$.

E_{BH} [eV]	Intensity [au]	FCF [au]	Transition
0.5670	$2.494\ 071 \times 10^{-2}$	$1.579\ 263 \times 10^{-1}$	0(0)→1(0)
0.6330	$5.634\ 408 \times 10^{-3}$	$7.506\ 269 \times 10^{-2}$	0(0)→1(1v7)
0.6478	$1.523\ 071 \times 10^{-3}$	$3.902\ 654 \times 10^{-2}$	0(0)→1(1v9)
0.6756	$2.739\ 918 \times 10^{-2}$	$1.655\ 270 \times 10^{-1}$	0(0)→1(1v8)
0.6842	$2.875\ 963 \times 10^{-2}$	$-1.695\ 866 \times 10^{-1}$	0(0)→1(1v6)

Continued on next page

Table S5: Table S5 – Continued from previous page

E_{BH} [eV]	Intensity [au]	FCF [au]	Transition
0.6989	$1.029\ 376 \times 10^{-3}$	$3.208\ 390 \times 10^{-2}$	$0(0)\rightarrow1(2v7)$
0.7206	$2.595\ 634 \times 10^{-3}$	$5.094\ 736 \times 10^{-2}$	$0(0)\rightarrow1(1v5)$
0.7285	$1.042\ 241 \times 10^{-3}$	$3.228\ 376 \times 10^{-2}$	$0(0)\rightarrow1(2v9)$
0.7301	$1.063\ 235 \times 10^{-2}$	$-1.031\ 133 \times 10^{-1}$	$0(0)\rightarrow1(1v4)$
0.7416	$5.450\ 907 \times 10^{-3}$	$7.383\ 026 \times 10^{-2}$	$0(0)\rightarrow1(1v7,1v8)$
0.7501	$6.244\ 429 \times 10^{-3}$	$-7.902\ 170 \times 10^{-2}$	$0(0)\rightarrow1(1v7,1v6)$
0.7516	$2.734\ 344 \times 10^{-3}$	$5.229\ 096 \times 10^{-2}$	$0(0)\rightarrow1(1v3)$
0.7564	$9.948\ 150 \times 10^{-4}$	$3.154\ 069 \times 10^{-2}$	$0(0)\rightarrow1(1v9,1v8)$
0.7649	$1.995\ 556 \times 10^{-3}$	$-4.467\ 164 \times 10^{-2}$	$0(0)\rightarrow1(1v9,1v6)$
0.7843	$1.913\ 721 \times 10^{-2}$	$1.383\ 373 \times 10^{-1}$	$0(0)\rightarrow1(2v8)$
0.7866	$8.349\ 666 \times 10^{-4}$	$2.889\ 579 \times 10^{-2}$	$0(0)\rightarrow1(1v7,1v5)$
0.7928	$2.983\ 042 \times 10^{-2}$	$-1.727\ 148 \times 10^{-1}$	$0(0)\rightarrow1(1v8,1v6)$
0.7961	$2.198\ 228 \times 10^{-3}$	$-4.688\ 526 \times 10^{-2}$	$0(0)\rightarrow1(1v7,1v4)$
0.8014	$1.948\ 531 \times 10^{-2}$	$1.395\ 898 \times 10^{-1}$	$0(0)\rightarrow1(2v6)$
0.8076	$9.224\ 151 \times 10^{-4}$	$3.037\ 129 \times 10^{-2}$	$0(0)\rightarrow1(2v7,1v8)$
0.8109	$5.766\ 484 \times 10^{-4}$	$-2.401\ 350 \times 10^{-2}$	$0(0)\rightarrow1(1v9,1v4)$
0.8161	$1.114\ 799 \times 10^{-3}$	$-3.338\ 860 \times 10^{-2}$	$0(0)\rightarrow1(2v7,1v6)$
0.8176	$5.241\ 314 \times 10^{-4}$	$2.289\ 392 \times 10^{-2}$	$0(0)\rightarrow1(1v7,1v3)$
0.8292	$3.204\ 468 \times 10^{-3}$	$5.660\ 802 \times 10^{-2}$	$0(0)\rightarrow1(1v8,1v5)$
0.8309	$6.163\ 621 \times 10^{-4}$	$-2.482\ 664 \times 10^{-2}$	$0(0)\rightarrow1(1v9,1v7,1v6)$
0.8372	$9.342\ 162 \times 10^{-4}$	$3.056\ 495 \times 10^{-2}$	$0(0)\rightarrow1(2v9,1v8)$
0.8378	$3.426\ 701 \times 10^{-3}$	$-5.853\ 803 \times 10^{-2}$	$0(0)\rightarrow1(1v6,1v5)$
0.8388	$1.106\ 530 \times 10^{-2}$	$-1.051\ 917 \times 10^{-1}$	$0(0)\rightarrow1(1v8,1v4)$
0.8457	$1.269\ 727 \times 10^{-3}$	$-3.563\ 322 \times 10^{-2}$	$0(0)\rightarrow1(2v9,1v6)$
0.8473	$1.292\ 793 \times 10^{-2}$	$1.137\ 011 \times 10^{-1}$	$0(0)\rightarrow1(1v6,1v4)$
0.8502	$3.430\ 479 \times 10^{-3}$	$5.857\ 029 \times 10^{-2}$	$0(0)\rightarrow1(1v7,2v8)$
0.8588	$5.659\ 486 \times 10^{-3}$	$-7.522\ 956 \times 10^{-2}$	$0(0)\rightarrow1(1v7,1v8,1v6)$
0.8603	$3.798\ 860 \times 10^{-3}$	$6.163\ 489 \times 10^{-2}$	$0(0)\rightarrow1(1v8,1v3)$
0.8673	$4.088\ 714 \times 10^{-3}$	$6.394\ 305 \times 10^{-2}$	$0(0)\rightarrow1(1v7,2v6)$
0.8688	$3.480\ 573 \times 10^{-3}$	$-5.899\ 638 \times 10^{-2}$	$0(0)\rightarrow1(1v6,1v3)$
0.8736	$1.261\ 825 \times 10^{-3}$	$-3.552\ 217 \times 10^{-2}$	$0(0)\rightarrow1(1v9,1v8,1v6)$
0.8821	$1.497\ 083 \times 10^{-3}$	$3.869\ 216 \times 10^{-2}$	$0(0)\rightarrow1(1v9,2v6)$
0.8837	$1.066\ 484 \times 10^{-3}$	$-3.265\ 707 \times 10^{-2}$	$0(0)\rightarrow1(1v5,1v4)$
0.8929	$1.054\ 001 \times 10^{-2}$	$1.026\ 646 \times 10^{-1}$	$0(0)\rightarrow1(3v8)$
0.8933	$2.558\ 704 \times 10^{-3}$	$5.058\ 364 \times 10^{-2}$	$0(0)\rightarrow1(2v4)$
0.8952	$9.149\ 745 \times 10^{-4}$	$3.024\ 855 \times 10^{-2}$	$0(0)\rightarrow1(1v7,1v8,1v5)$
0.9015	$1.990\ 639 \times 10^{-2}$	$-1.410\ 900 \times 10^{-1}$	$0(0)\rightarrow1(2v8,1v6)$
0.9037	$1.045\ 778 \times 10^{-3}$	$-3.233\ 848 \times 10^{-2}$	$0(0)\rightarrow1(1v7,1v6,1v5)$
0.9047	$1.989\ 827 \times 10^{-3}$	$-4.460\ 747 \times 10^{-2}$	$0(0)\rightarrow1(1v7,1v8,1v4)$
0.9100	$1.922\ 762 \times 10^{-2}$	$1.386\ 637 \times 10^{-1}$	$0(0)\rightarrow1(1v8,2v6)$
0.9133	$2.573\ 238 \times 10^{-3}$	$5.072\ 710 \times 10^{-2}$	$0(0)\rightarrow1(1v7,1v6,1v4)$
0.9148	$1.247\ 227 \times 10^{-3}$	$-3.531\ 610 \times 10^{-2}$	$0(0)\rightarrow1(1v4,1v3)$
0.9162	$5.487\ 538 \times 10^{-4}$	$2.342\ 549 \times 10^{-2}$	$0(0)\rightarrow1(2v7,2v8)$
0.9186	$9.991\ 816 \times 10^{-3}$	$-9.995\ 907 \times 10^{-2}$	$0(0)\rightarrow1(3v6)$
0.9248	$9.329\ 596 \times 10^{-4}$	$-3.054\ 439 \times 10^{-2}$	$0(0)\rightarrow1(2v7,1v8,1v6)$
0.9262	$6.572\ 315 \times 10^{-4}$	$2.563\ 653 \times 10^{-2}$	$0(0)\rightarrow1(1v7,1v8,1v3)$
0.9281	$8.023\ 621 \times 10^{-4}$	$2.832\ 600 \times 10^{-2}$	$0(0)\rightarrow1(1v9,1v6,1v4)$
0.9333	$7.160\ 158 \times 10^{-4}$	$2.675\ 847 \times 10^{-2}$	$0(0)\rightarrow1(2v7,2v6)$
0.9348	$6.457\ 742 \times 10^{-4}$	$-2.541\ 209 \times 10^{-2}$	$0(0)\rightarrow1(1v7,1v6,1v3)$
0.9379	$2.438\ 783 \times 10^{-3}$	$4.938\ 404 \times 10^{-2}$	$0(0)\rightarrow1(2v8,1v5)$
0.9458	$5.752\ 186 \times 10^{-4}$	$2.398\ 371 \times 10^{-2}$	$0(0)\rightarrow1(2v9,2v8)$

Continued on next page

Table S5: Table S5 – Continued from previous page

E_{BH} [eV]	Intensity [au]	FCF [au]	Transition
0.9464	$3.991\,340 \times 10^{-3}$	$-6.317\,705 \times 10^{-2}$	$0(0)\rightarrow1(1v8,1v6,1v5)$
0.9474	$7.404\,273 \times 10^{-3}$	$-8.604\,809 \times 10^{-2}$	$0(0)\rightarrow1(2v8,1v4)$
0.9544	$1.061\,017 \times 10^{-3}$	$-3.257\,325 \times 10^{-2}$	$0(0)\rightarrow1(2v9,1v8,1v6)$
0.9550	$2.585\,400 \times 10^{-3}$	$5.084\,683 \times 10^{-2}$	$0(0)\rightarrow1(2v6,1v5)$
0.9560	$1.272\,149 \times 10^{-2}$	$1.127\,896 \times 10^{-1}$	$0(0)\rightarrow1(1v8,1v6,1v4)$
0.9589	$1.717\,748 \times 10^{-3}$	$4.144\,572 \times 10^{-2}$	$0(0)\rightarrow1(1v7,3v8)$
0.9629	$9.030\,295 \times 10^{-4}$	$3.005\,045 \times 10^{-2}$	$0(0)\rightarrow1(2v9,2v6)$
0.9645	$9.150\,493 \times 10^{-3}$	$-9.565\,821 \times 10^{-2}$	$0(0)\rightarrow1(2v6,1v4)$
0.9674	$3.384\,912 \times 10^{-3}$	$-5.818\,000 \times 10^{-2}$	$0(0)\rightarrow1(1v7,2v8,1v6)$
0.9689	$3.127\,578 \times 10^{-3}$	$5.592\,475 \times 10^{-2}$	$0(0)\rightarrow1(2v8,1v3)$
0.9760	$3.501\,801 \times 10^{-3}$	$5.917\,602 \times 10^{-2}$	$0(0)\rightarrow1(1v7,1v8,2v6)$
0.9775	$4.556\,307 \times 10^{-3}$	$-6.750\,042 \times 10^{-2}$	$0(0)\rightarrow1(1v8,1v6,1v3)$
0.9822	$5.200\,151 \times 10^{-4}$	$-2.280\,384 \times 10^{-2}$	$0(0)\rightarrow1(1v9,2v8,1v6)$
0.9845	$2.032\,836 \times 10^{-3}$	$-4.508\,698 \times 10^{-2}$	$0(0)\rightarrow1(1v7,3v6)$
0.9860	$2.554\,232 \times 10^{-3}$	$5.053\,941 \times 10^{-2}$	$0(0)\rightarrow1(2v6,1v3)$
0.9908	$9.159\,001 \times 10^{-4}$	$3.026\,384 \times 10^{-2}$	$0(0)\rightarrow1(1v9,1v8,2v6)$
0.9924	$1.252\,689 \times 10^{-3}$	$-3.539\,335 \times 10^{-2}$	$0(0)\rightarrow1(1v8,1v5,1v4)$
0.9993	$8.371\,008 \times 10^{-4}$	$-2.893\,269 \times 10^{-2}$	$0(0)\rightarrow1(1v9,3v6)$
1.0009	$1.484\,399 \times 10^{-3}$	$3.852\,790 \times 10^{-2}$	$0(0)\rightarrow1(1v6,1v5,1v4)$
1.0016	$4.984\,658 \times 10^{-3}$	$7.060\,211 \times 10^{-2}$	$0(0)\rightarrow1(4v8)$
1.0019	$2.535\,624 \times 10^{-3}$	$5.035\,498 \times 10^{-2}$	$0(0)\rightarrow1(1v8,2v4)$
1.0039	$6.308\,203 \times 10^{-4}$	$2.511\,614 \times 10^{-2}$	$0(0)\rightarrow1(1v7,2v8,1v5)$
1.0088	$5.422\,650 \times 10^{-4}$	$2.328\,658 \times 10^{-2}$	$0(0)\rightarrow1(2v9,1v6,1v4)$
1.0101	$1.052\,832 \times 10^{-2}$	$-1.026\,076 \times 10^{-1}$	$0(0)\rightarrow1(3v8,1v6)$
1.0104	$3.256\,416 \times 10^{-3}$	$-5.706\,501 \times 10^{-2}$	$0(0)\rightarrow1(1v6,2v4)$
1.0124	$1.074\,757 \times 10^{-3}$	$-3.278\,348 \times 10^{-2}$	$0(0)\rightarrow1(1v7,1v8,1v6,1v5)$
1.0134	$1.188\,439 \times 10^{-3}$	$-3.447\,374 \times 10^{-2}$	$0(0)\rightarrow1(1v7,2v8,1v4)$
1.0187	$1.234\,426 \times 10^{-2}$	$1.111\,047 \times 10^{-1}$	$0(0)\rightarrow1(2v8,2v6)$
1.0209	$7.548\,573 \times 10^{-4}$	$2.747\,467 \times 10^{-2}$	$0(0)\rightarrow1(1v7,2v6,1v5)$
1.0219	$2.184\,878 \times 10^{-3}$	$4.674\,268 \times 10^{-2}$	$0(0)\rightarrow1(1v7,1v8,1v6,1v4)$
1.0234	$1.641\,748 \times 10^{-3}$	$-4.051\,849 \times 10^{-2}$	$0(0)\rightarrow1(1v8,1v4,1v3)$
1.0272	$9.421\,348 \times 10^{-3}$	$-9.706\,363 \times 10^{-2}$	$0(0)\rightarrow1(1v8,3v6)$
1.0305	$1.762\,033 \times 10^{-3}$	$-4.197\,658 \times 10^{-2}$	$0(0)\rightarrow1(1v7,2v6,1v4)$
1.0319	$1.661\,851 \times 10^{-3}$	$4.076\,580 \times 10^{-2}$	$0(0)\rightarrow1(1v6,1v4,1v3)$
1.0334	$5.269\,648 \times 10^{-4}$	$-2.295\,571 \times 10^{-2}$	$0(0)\rightarrow1(2v7,2v8,1v6)$
1.0357	$4.274\,924 \times 10^{-3}$	$6.538\,290 \times 10^{-2}$	$0(0)\rightarrow1(4v6)$
1.0419	$5.648\,697 \times 10^{-4}$	$2.376\,699 \times 10^{-2}$	$0(0)\rightarrow1(2v7,1v8,2v6)$
1.0434	$7.568\,890 \times 10^{-4}$	$-2.751\,162 \times 10^{-2}$	$0(0)\rightarrow1(1v7,1v8,1v6,1v3)$
1.0453	$6.327\,986 \times 10^{-4}$	$-2.515\,549 \times 10^{-2}$	$0(0)\rightarrow1(1v9,2v6,1v4)$
1.0465	$1.443\,090 \times 10^{-3}$	$3.798\,803 \times 10^{-2}$	$0(0)\rightarrow1(3v8,1v5)$
1.0551	$2.897\,957 \times 10^{-3}$	$-5.383\,267 \times 10^{-2}$	$0(0)\rightarrow1(2v8,1v6,1v5)$
1.0561	$3.925\,760 \times 10^{-3}$	$-6.265\,589 \times 10^{-2}$	$0(0)\rightarrow1(3v8,1v4)$
1.0572	$1.457\,639 \times 10^{-3}$	$-3.817\,903 \times 10^{-2}$	$0(0)\rightarrow1(1v9,1v1)$
1.0630	$6.189\,798 \times 10^{-4}$	$-2.487\,930 \times 10^{-2}$	$0(0)\rightarrow1(2v9,2v8,1v6)$
1.0636	$2.861\,335 \times 10^{-3}$	$5.349\,144 \times 10^{-2}$	$0(0)\rightarrow1(1v8,2v6,1v5)$
1.0646	$8.147\,827 \times 10^{-3}$	$9.026\,531 \times 10^{-2}$	$0(0)\rightarrow1(2v8,1v6,1v4)$
1.0649	$1.205\,411 \times 10^{-3}$	$3.471\,903 \times 10^{-2}$	$0(0)\rightarrow1(1v8,1v2)$
1.0675	$7.429\,983 \times 10^{-4}$	$2.725\,800 \times 10^{-2}$	$0(0)\rightarrow1(1v7,4v8)$
1.0715	$7.100\,090 \times 10^{-4}$	$2.664\,599 \times 10^{-2}$	$0(0)\rightarrow1(2v9,1v8,2v6)$
1.0722	$1.452\,298 \times 10^{-3}$	$-3.810\,903 \times 10^{-2}$	$0(0)\rightarrow1(3v6,1v5)$
1.0731	$8.572\,458 \times 10^{-3}$	$-9.258\,757 \times 10^{-2}$	$0(0)\rightarrow1(1v8,2v6,1v4)$

Continued on next page

Table S5: Table S5 – Continued from previous page

E_{BH} [eV]	Intensity [au]	FCF [au]	Transition
1.0761	$1.619\ 512 \times 10^{-3}$	$-4.024\ 317 \times 10^{-2}$	$0(0) \rightarrow 1(1v7,3v8,1v6)$
1.0764	$5.979\ 348 \times 10^{-4}$	$-2.445\ 271 \times 10^{-2}$	$0(0) \rightarrow 1(1v7,1v6,2v4)$
1.0776	$1.967\ 069 \times 10^{-3}$	$4.435\ 165 \times 10^{-2}$	$0(0) \rightarrow 1(3v8,1v3)$
1.0817	$4.874\ 711 \times 10^{-3}$	$6.981\ 913 \times 10^{-2}$	$0(0) \rightarrow 1(3v6,1v4)$
1.0846	$2.006\ 310 \times 10^{-3}$	$4.479\ 185 \times 10^{-2}$	$0(0) \rightarrow 1(1v7,2v8,2v6)$
1.0861	$3.572\ 140 \times 10^{-3}$	$-5.976\ 738 \times 10^{-2}$	$0(0) \rightarrow 1(2v8,1v6,1v3)$
1.0932	$1.653\ 251 \times 10^{-3}$	$-4.066\ 019 \times 10^{-2}$	$0(0) \rightarrow 1(1v7,1v8,3v6)$
1.0946	$3.174\ 987 \times 10^{-3}$	$5.634\ 702 \times 10^{-2}$	$0(0) \rightarrow 1(1v8,2v6,1v3)$
1.1010	$9.150\ 417 \times 10^{-4}$	$-3.024\ 966 \times 10^{-2}$	$0(0) \rightarrow 1(2v8,1v5,1v4)$
1.1017	$8.452\ 092 \times 10^{-4}$	$2.907\ 248 \times 10^{-2}$	$0(0) \rightarrow 1(1v7,4v6)$
1.1032	$1.402\ 676 \times 10^{-3}$	$-3.745\ 231 \times 10^{-2}$	$0(0) \rightarrow 1(3v6,1v3)$
1.1096	$1.646\ 926 \times 10^{-3}$	$4.058\ 233 \times 10^{-2}$	$0(0) \rightarrow 1(1v8,1v6,1v5,1v4)$
1.1102	$2.113\ 242 \times 10^{-3}$	$4.597\ 001 \times 10^{-2}$	$0(0) \rightarrow 1(5v8)$
1.1105	$1.633\ 327 \times 10^{-3}$	$4.041\ 445 \times 10^{-2}$	$0(0) \rightarrow 1(2v8,2v4)$
1.1181	$1.171\ 091 \times 10^{-3}$	$-3.422\ 121 \times 10^{-2}$	$0(0) \rightarrow 1(2v6,1v5,1v4)$
1.1188	$4.798\ 387 \times 10^{-3}$	$-6.927\ 039 \times 10^{-2}$	$0(0) \rightarrow 1(4v8,1v6)$
1.1191	$3.053\ 950 \times 10^{-3}$	$-5.526\ 255 \times 10^{-2}$	$0(0) \rightarrow 1(1v8,1v6,2v4)$
1.1210	$7.039\ 515 \times 10^{-4}$	$-2.653\ 208 \times 10^{-2}$	$0(0) \rightarrow 1(1v7,2v8,1v6,1v5)$
1.1220	$5.677\ 181 \times 10^{-4}$	$-2.382\ 684 \times 10^{-2}$	$0(0) \rightarrow 1(1v7,3v8,1v4)$
1.1273	$6.310\ 346 \times 10^{-3}$	$7.943\ 768 \times 10^{-2}$	$0(0) \rightarrow 1(3v8,2v6)$
1.1276	$2.394\ 883 \times 10^{-3}$	$4.893\ 754 \times 10^{-2}$	$0(0) \rightarrow 1(2v6,2v4)$
1.1296	$7.332\ 451 \times 10^{-4}$	$2.707\ 850 \times 10^{-2}$	$0(0) \rightarrow 1(1v7,1v8,2v6,1v5)$
1.1306	$1.242\ 485 \times 10^{-3}$	$3.524\ 890 \times 10^{-2}$	$0(0) \rightarrow 1(1v7,2v8,1v6,1v4)$
1.1311	$5.561\ 488 \times 10^{-4}$	$-2.358\ 281 \times 10^{-2}$	$0(0) \rightarrow 1(1v8,1v6,1v5,1v3)$
1.1320	$1.292\ 486 \times 10^{-3}$	$-3.595\ 116 \times 10^{-2}$	$0(0) \rightarrow 1(2v8,1v4,1v3)$
1.1358	$5.842\ 437 \times 10^{-3}$	$-7.643\ 583 \times 10^{-2}$	$0(0) \rightarrow 1(2v8,3v6)$
1.1391	$1.414\ 344 \times 10^{-3}$	$-3.760\ 776 \times 10^{-2}$	$0(0) \rightarrow 1(1v7,1v8,2v6,1v4)$
1.1406	$2.064\ 801 \times 10^{-3}$	$4.544\ 008 \times 10^{-2}$	$0(0) \rightarrow 1(1v8,1v6,1v4,1v3)$
1.1444	$3.863\ 561 \times 10^{-3}$	$6.215\ 755 \times 10^{-2}$	$0(0) \rightarrow 1(1v8,4v6)$
1.1476	$9.107\ 960 \times 10^{-4}$	$3.017\ 940 \times 10^{-2}$	$0(0) \rightarrow 1(1v7,3v6,1v4)$
1.1491	$1.267\ 901 \times 10^{-3}$	$-3.560\ 760 \times 10^{-2}$	$0(0) \rightarrow 1(2v6,1v4,1v3)$
1.1521	$5.367\ 175 \times 10^{-4}$	$-2.316\ 716 \times 10^{-2}$	$0(0) \rightarrow 1(1v7,2v8,1v6,1v3)$
1.1529	$1.604\ 950 \times 10^{-3}$	$-4.006\ 182 \times 10^{-2}$	$0(0) \rightarrow 1(5v6)$
1.1552	$7.262\ 036 \times 10^{-4}$	$2.694\ 817 \times 10^{-2}$	$0(0) \rightarrow 1(4v8,1v5)$
1.1606	$5.086\ 544 \times 10^{-4}$	$2.255\ 337 \times 10^{-2}$	$0(0) \rightarrow 1(1v7,1v8,2v6,1v3)$
1.1637	$1.644\ 763 \times 10^{-3}$	$-4.055\ 568 \times 10^{-2}$	$0(0) \rightarrow 1(3v8,1v6,1v5)$
1.1647	$1.793\ 326 \times 10^{-3}$	$-4.234\ 768 \times 10^{-2}$	$0(0) \rightarrow 1(4v8,1v4)$
1.1658	$1.469\ 467 \times 10^{-3}$	$-3.833\ 363 \times 10^{-2}$	$0(0) \rightarrow 1(1v9,1v8,1v1)$
1.1723	$1.994\ 930 \times 10^{-3}$	$4.466\ 464 \times 10^{-2}$	$0(0) \rightarrow 1(2v8,2v6,1v5)$
1.1732	$4.155\ 773 \times 10^{-3}$	$6.446\ 528 \times 10^{-2}$	$0(0) \rightarrow 1(3v8,1v6,1v4)$
1.1736	$6.020\ 699 \times 10^{-4}$	$2.453\ 711 \times 10^{-2}$	$0(0) \rightarrow 1(1v6,3v4)$
1.1736	$2.123\ 509 \times 10^{-3}$	$4.608\ 154 \times 10^{-2}$	$0(0) \rightarrow 1(2v8,1v2)$
1.1743	$1.708\ 268 \times 10^{-3}$	$4.133\ 120 \times 10^{-2}$	$0(0) \rightarrow 1(1v9,1v6,1v1)$
1.1808	$1.534\ 052 \times 10^{-3}$	$-3.916\ 698 \times 10^{-2}$	$0(0) \rightarrow 1(1v8,3v6,1v5)$
1.1818	$5.288\ 105 \times 10^{-3}$	$-7.271\ 935 \times 10^{-2}$	$0(0) \rightarrow 1(2v8,2v6,1v4)$
1.1821	$1.547\ 056 \times 10^{-3}$	$-3.933\ 263 \times 10^{-2}$	$0(0) \rightarrow 1(1v8,1v6,1v2)$
1.1847	$6.718\ 852 \times 10^{-4}$	$-2.592\ 075 \times 10^{-2}$	$0(0) \rightarrow 1(1v7,4v8,1v6)$
1.1862	$1.040\ 294 \times 10^{-3}$	$3.225\ 359 \times 10^{-2}$	$0(0) \rightarrow 1(4v8,1v3)$
1.1893	$6.728\ 731 \times 10^{-4}$	$2.593\ 980 \times 10^{-2}$	$0(0) \rightarrow 1(4v6,1v5)$
1.1903	$4.365\ 628 \times 10^{-3}$	$6.607\ 290 \times 10^{-2}$	$0(0) \rightarrow 1(1v8,3v6,1v4)$
1.1933	$9.240\ 582 \times 10^{-4}$	$3.039\ 832 \times 10^{-2}$	$0(0) \rightarrow 1(1v7,3v8,2v6)$

Continued on next page

Table S5: Table S5 – Continued from previous page

E_{BH} [eV]	Intensity [au]	FCF [au]	Transition
1.1947	$2.151\ 855 \times 10^{-3}$	$-4.638\ 809 \times 10^{-2}$	$0(0)\rightarrow1(3v8,1v6,1v3)$
1.1989	$2.158\ 090 \times 10^{-3}$	$-4.645\ 525 \times 10^{-2}$	$0(0)\rightarrow1(4v6,1v4)$
1.2018	$9.114\ 148 \times 10^{-4}$	$-3.018\ 965 \times 10^{-2}$	$0(0)\rightarrow1(1v7,2v8,3v6)$
1.2033	$2.387\ 240 \times 10^{-3}$	$4.885\ 939 \times 10^{-2}$	$0(0)\rightarrow1(2v8,2v6,1v3)$
1.2097	$5.219\ 449 \times 10^{-4}$	$-2.284\ 611 \times 10^{-2}$	$0(0)\rightarrow1(3v8,1v5,1v4)$
1.2103	$6.549\ 313 \times 10^{-4}$	$2.559\ 163 \times 10^{-2}$	$0(0)\rightarrow1(1v7,1v8,4v6)$
1.2118	$1.663\ 499 \times 10^{-3}$	$-4.078\ 602 \times 10^{-2}$	$0(0)\rightarrow1(1v8,3v6,1v3)$
1.2182	$1.149\ 491 \times 10^{-3}$	$3.390\ 415 \times 10^{-2}$	$0(0)\rightarrow1(2v8,1v6,1v5,1v4)$
1.2189	$8.241\ 443 \times 10^{-4}$	$2.870\ 791 \times 10^{-2}$	$0(0)\rightarrow1(6v8)$
1.2192	$8.374\ 324 \times 10^{-4}$	$2.893\ 843 \times 10^{-2}$	$0(0)\rightarrow1(3v8,2v4)$
1.2203	$6.398\ 558 \times 10^{-4}$	$2.529\ 537 \times 10^{-2}$	$0(0)\rightarrow1(1v9,1v4,1v1)$
1.2204	$6.375\ 547 \times 10^{-4}$	$2.524\ 985 \times 10^{-2}$	$0(0)\rightarrow1(4v6,1v3)$
1.2267	$1.235\ 274 \times 10^{-3}$	$-3.514\ 646 \times 10^{-2}$	$0(0)\rightarrow1(1v8,2v6,1v5,1v4)$
1.2274	$1.965\ 349 \times 10^{-3}$	$-4.433\ 226 \times 10^{-2}$	$0(0)\rightarrow1(5v8,1v6)$
1.2277	$1.885\ 351 \times 10^{-3}$	$-4.342\ 063 \times 10^{-2}$	$0(0)\rightarrow1(2v8,1v6,2v4)$
1.2353	$6.841\ 581 \times 10^{-4}$	$2.615\ 642 \times 10^{-2}$	$0(0)\rightarrow1(3v6,1v5,1v4)$
1.2359	$2.788\ 909 \times 10^{-3}$	$5.281\ 012 \times 10^{-2}$	$0(0)\rightarrow1(4v8,2v6)$
1.2363	$2.139\ 057 \times 10^{-3}$	$4.624\ 994 \times 10^{-2}$	$0(0)\rightarrow1(1v8,2v6,2v4)$
1.2392	$5.681\ 265 \times 10^{-4}$	$2.383\ 540 \times 10^{-2}$	$0(0)\rightarrow1(1v7,3v8,1v6,1v4)$
1.2395	$5.974\ 229 \times 10^{-4}$	$2.444\ 224 \times 10^{-2}$	$0(0)\rightarrow1(1v7,2v8,1v2)$
1.2407	$7.813\ 396 \times 10^{-4}$	$-2.795\ 245 \times 10^{-2}$	$0(0)\rightarrow1(3v8,1v4,1v3)$
1.2445	$2.897\ 225 \times 10^{-3}$	$-5.382\ 588 \times 10^{-2}$	$0(0)\rightarrow1(3v8,3v6)$
1.2448	$1.319\ 568 \times 10^{-3}$	$-3.632\ 586 \times 10^{-2}$	$0(0)\rightarrow1(3v6,2v4)$
1.2477	$7.712\ 887 \times 10^{-4}$	$-2.777\ 208 \times 10^{-2}$	$0(0)\rightarrow1(1v7,2v8,2v6,1v4)$
1.2481	$5.321\ 856 \times 10^{-4}$	$-2.306\ 915 \times 10^{-2}$	$0(0)\rightarrow1(1v7,1v8,1v6,1v2)$
1.2492	$1.550\ 973 \times 10^{-3}$	$3.938\ 240 \times 10^{-2}$	$0(0)\rightarrow1(2v8,1v6,1v4,1v3)$
1.2530	$2.320\ 834 \times 10^{-3}$	$4.817\ 503 \times 10^{-2}$	$0(0)\rightarrow1(2v8,4v6)$
1.2563	$6.942\ 741 \times 10^{-4}$	$2.634\ 908 \times 10^{-2}$	$0(0)\rightarrow1(1v7,1v8,3v6,1v4)$
1.2578	$1.497\ 392 \times 10^{-3}$	$-3.869\ 615 \times 10^{-2}$	$0(0)\rightarrow1(1v8,2v6,1v4,1v3)$
1.2616	$1.393\ 528 \times 10^{-3}$	$-3.732\ 999 \times 10^{-2}$	$0(0)\rightarrow1(1v8,5v6)$
1.2663	$7.206\ 741 \times 10^{-4}$	$2.684\ 537 \times 10^{-2}$	$0(0)\rightarrow1(3v6,1v4,1v3)$
1.2701	$5.450\ 301 \times 10^{-4}$	$2.334\ 588 \times 10^{-2}$	$0(0)\rightarrow1(6v6)$
1.2724	$7.968\ 214 \times 10^{-4}$	$-2.822\ 802 \times 10^{-2}$	$0(0)\rightarrow1(4v8,1v6,1v5)$
1.2733	$7.361\ 233 \times 10^{-4}$	$-2.713\ 159 \times 10^{-2}$	$0(0)\rightarrow1(5v8,1v4)$
1.2744	$9.953\ 026 \times 10^{-4}$	$-3.154\ 842 \times 10^{-2}$	$0(0)\rightarrow1(1v9,2v8,1v1)$
1.2809	$1.092\ 626 \times 10^{-3}$	$3.305\ 490 \times 10^{-2}$	$0(0)\rightarrow1(3v8,2v6,1v5)$
1.2819	$1.832\ 699 \times 10^{-3}$	$4.281\ 003 \times 10^{-2}$	$0(0)\rightarrow1(4v8,1v6,1v4)$
1.2822	$5.398\ 013 \times 10^{-4}$	$2.323\ 362 \times 10^{-2}$	$0(0)\rightarrow1(1v8,1v6,3v4)$
1.2822	$2.043\ 919 \times 10^{-3}$	$4.520\ 972 \times 10^{-2}$	$0(0)\rightarrow1(3v8,1v2)$
1.2830	$1.606\ 832 \times 10^{-3}$	$4.008\ 531 \times 10^{-2}$	$0(0)\rightarrow1(1v9,1v8,1v6,1v1)$
1.2894	$1.031\ 252 \times 10^{-3}$	$-3.211\ 312 \times 10^{-2}$	$0(0)\rightarrow1(2v8,3v6,1v5)$
1.2904	$2.609\ 689 \times 10^{-3}$	$-5.108\ 512 \times 10^{-2}$	$0(0)\rightarrow1(3v8,2v6,1v4)$
1.2908	$2.484\ 412 \times 10^{-3}$	$-4.984\ 388 \times 10^{-2}$	$0(0)\rightarrow1(2v8,1v6,1v2)$
1.2915	$1.175\ 673 \times 10^{-3}$	$-3.428\ 808 \times 10^{-2}$	$0(0)\rightarrow1(1v9,2v6,1v1)$
1.2980	$6.805\ 475 \times 10^{-4}$	$2.608\ 731 \times 10^{-2}$	$0(0)\rightarrow1(1v8,4v6,1v5)$
1.2990	$2.603\ 466 \times 10^{-3}$	$5.102\ 417 \times 10^{-2}$	$0(0)\rightarrow1(2v8,3v6,1v4)$
1.2993	$1.135\ 841 \times 10^{-3}$	$3.370\ 224 \times 10^{-2}$	$0(0)\rightarrow1(1v8,2v6,1v2)$
1.3034	$1.094\ 247 \times 10^{-3}$	$-3.307\ 940 \times 10^{-2}$	$0(0)\rightarrow1(4v8,1v6,1v3)$
1.3037	$5.224\ 871 \times 10^{-4}$	$-2.285\ 798 \times 10^{-2}$	$0(0)\rightarrow1(1v8,1v6,2v4,1v3)$
1.3075	$1.852\ 977 \times 10^{-3}$	$-4.304\ 622 \times 10^{-2}$	$0(0)\rightarrow1(1v8,4v6,1v4)$
1.3119	$1.386\ 489 \times 10^{-3}$	$3.723\ 559 \times 10^{-2}$	$0(0)\rightarrow1(3v8,2v6,1v3)$

Continued on next page

Table S5: Table S5 – Continued from previous page

E_{BH} [eV]	Intensity [au]	FCF [au]	Transition
1.3161	$8.358\,369 \times 10^{-4}$	$2.891\,084 \times 10^{-2}$	$0(0)\rightarrow1(5v6,1v4)$
1.3205	$1.204\,721 \times 10^{-3}$	$-3.470\,910 \times 10^{-2}$	$0(0)\rightarrow1(2v8,3v6,1v3)$
1.3268	$6.298\,888 \times 10^{-4}$	$2.509\,758 \times 10^{-2}$	$0(0)\rightarrow1(3v8,1v6,1v5,1v4)$
1.3289	$6.099\,998 \times 10^{-4}$	$2.469\,817 \times 10^{-2}$	$0(0)\rightarrow1(1v9,1v8,1v4,1v1)$
1.3290	$7.238\,332 \times 10^{-4}$	$2.690\,415 \times 10^{-2}$	$0(0)\rightarrow1(1v8,4v6,1v3)$
1.3354	$8.287\,162 \times 10^{-4}$	$-2.878\,743 \times 10^{-2}$	$0(0)\rightarrow1(2v8,2v6,1v5,1v4)$
1.3361	$7.419\,347 \times 10^{-4}$	$-2.723\,848 \times 10^{-2}$	$0(0)\rightarrow1(6v8,1v6)$
1.3364	$9.310\,346 \times 10^{-4}$	$-3.051\,286 \times 10^{-2}$	$0(0)\rightarrow1(3v8,1v6,2v4)$
1.3367	$7.939\,581 \times 10^{-4}$	$-2.817\,726 \times 10^{-2}$	$0(0)\rightarrow1(2v8,1v4,1v2)$
1.3375	$7.902\,473 \times 10^{-4}$	$-2.811\,134 \times 10^{-2}$	$0(0)\rightarrow1(1v9,1v6,1v4,1v1)$
1.3439	$6.889\,895 \times 10^{-4}$	$2.624\,861 \times 10^{-2}$	$0(0)\rightarrow1(1v8,3v6,1v5,1v4)$
1.3446	$1.110\,272 \times 10^{-3}$	$3.332\,074 \times 10^{-2}$	$0(0)\rightarrow1(5v8,2v6)$
1.3449	$1.272\,892 \times 10^{-3}$	$3.567\,761 \times 10^{-2}$	$0(0)\rightarrow1(2v8,2v6,2v4)$
1.3452	$6.186\,973 \times 10^{-4}$	$2.487\,363 \times 10^{-2}$	$0(0)\rightarrow1(1v8,1v6,1v4,1v2)$
1.3531	$1.245\,923 \times 10^{-3}$	$-3.529\,763 \times 10^{-2}$	$0(0)\rightarrow1(4v8,3v6)$
1.3535	$1.126\,893 \times 10^{-3}$	$-3.356\,923 \times 10^{-2}$	$0(0)\rightarrow1(1v8,3v6,2v4)$
1.3567	$6.578\,640 \times 10^{-4}$	$-2.564\,886 \times 10^{-2}$	$0(0)\rightarrow1(1v7,2v8,1v6,1v2)$
1.3579	$8.997\,283 \times 10^{-4}$	$2.999\,547 \times 10^{-2}$	$0(0)\rightarrow1(3v8,1v6,1v4,1v3)$
1.3617	$1.119\,296 \times 10^{-3}$	$3.345\,588 \times 10^{-2}$	$0(0)\rightarrow1(3v8,4v6)$
1.3620	$6.022\,243 \times 10^{-4}$	$2.454\,026 \times 10^{-2}$	$0(0)\rightarrow1(4v6,2v4)$
1.3664	$1.080\,050 \times 10^{-3}$	$-3.286\,411 \times 10^{-2}$	$0(0)\rightarrow1(2v8,2v6,1v4,1v3)$
1.3702	$8.126\,162 \times 10^{-4}$	$-2.850\,642 \times 10^{-2}$	$0(0)\rightarrow1(2v8,5v6)$
1.3750	$8.125\,901 \times 10^{-4}$	$2.850\,597 \times 10^{-2}$	$0(0)\rightarrow1(1v8,3v6,1v4,1v3)$
1.3831	$5.454\,356 \times 10^{-4}$	$-2.335\,456 \times 10^{-2}$	$0(0)\rightarrow1(1v9,3v8,1v1)$
1.3896	$5.125\,597 \times 10^{-4}$	$2.263\,978 \times 10^{-2}$	$0(0)\rightarrow1(4v8,2v6,1v5)$
1.3905	$7.280\,548 \times 10^{-4}$	$2.698\,249 \times 10^{-2}$	$0(0)\rightarrow1(5v8,1v6,1v4)$
1.3909	$1.434\,008 \times 10^{-3}$	$3.786\,829 \times 10^{-2}$	$0(0)\rightarrow1(4v8,1v2)$
1.3916	$1.032\,269 \times 10^{-3}$	$3.212\,894 \times 10^{-2}$	$0(0)\rightarrow1(1v9,2v8,1v6,1v1)$
1.3981	$5.470\,989 \times 10^{-4}$	$-2.339\,014 \times 10^{-2}$	$0(0)\rightarrow1(3v8,3v6,1v5)$
1.3991	$1.117\,192 \times 10^{-3}$	$-3.342\,442 \times 10^{-2}$	$0(0)\rightarrow1(4v8,2v6,1v4)$
1.3994	$2.249\,823 \times 10^{-3}$	$-4.743\,230 \times 10^{-2}$	$0(0)\rightarrow1(3v8,1v6,1v2)$
1.4002	$1.041\,178 \times 10^{-3}$	$-3.226\,728 \times 10^{-2}$	$0(0)\rightarrow1(1v9,1v8,2v6,1v1)$
1.4076	$1.247\,339 \times 10^{-3}$	$3.531\,768 \times 10^{-2}$	$0(0)\rightarrow1(3v8,3v6,1v4)$
1.4079	$1.692\,415 \times 10^{-3}$	$4.113\,898 \times 10^{-2}$	$0(0)\rightarrow1(2v8,2v6,1v2)$
1.4087	$6.121\,766 \times 10^{-4}$	$2.474\,220 \times 10^{-2}$	$0(0)\rightarrow1(1v9,3v6,1v1)$
1.4162	$1.071\,148 \times 10^{-3}$	$-3.272\,840 \times 10^{-2}$	$0(0)\rightarrow1(2v8,4v6,1v4)$
1.4165	$6.214\,929 \times 10^{-4}$	$-2.492\,976 \times 10^{-2}$	$0(0)\rightarrow1(1v8,3v6,1v2)$
1.4206	$6.821\,899 \times 10^{-4}$	$2.611\,877 \times 10^{-2}$	$0(0)\rightarrow1(4v8,2v6,1v3)$
1.4247	$6.895\,717 \times 10^{-4}$	$2.625\,970 \times 10^{-2}$	$0(0)\rightarrow1(1v8,5v6,1v4)$
1.4291	$6.772\,435 \times 10^{-4}$	$-2.602\,390 \times 10^{-2}$	$0(0)\rightarrow1(3v8,3v6,1v3)$
1.4377	$5.064\,710 \times 10^{-4}$	$2.250\,491 \times 10^{-2}$	$0(0)\rightarrow1(2v8,4v6,1v3)$
1.4453	$7.457\,520 \times 10^{-4}$	$-2.730\,846 \times 10^{-2}$	$0(0)\rightarrow1(3v8,1v4,1v2)$
1.4461	$7.040\,460 \times 10^{-4}$	$-2.653\,386 \times 10^{-2}$	$0(0)\rightarrow1(1v9,1v8,1v6,1v4,1v1)$
1.4536	$6.086\,454 \times 10^{-4}$	$2.467\,074 \times 10^{-2}$	$0(0)\rightarrow1(3v8,2v6,2v4)$
1.4539	$9.835\,989 \times 10^{-4}$	$3.136\,238 \times 10^{-2}$	$0(0)\rightarrow1(2v8,1v6,1v4,1v2)$
1.4547	$5.679\,067 \times 10^{-4}$	$2.383\,079 \times 10^{-2}$	$0(0)\rightarrow1(1v9,2v6,1v4,1v1)$
1.4621	$6.486\,771 \times 10^{-4}$	$-2.546\,914 \times 10^{-2}$	$0(0)\rightarrow1(2v8,3v6,2v4)$
1.4654	$5.037\,241 \times 10^{-4}$	$-2.244\,380 \times 10^{-2}$	$0(0)\rightarrow1(1v7,3v8,1v6,1v2)$
1.4751	$6.047\,977 \times 10^{-4}$	$-2.459\,263 \times 10^{-2}$	$0(0)\rightarrow1(3v8,2v6,1v4,1v3)$
1.4754	$5.204\,542 \times 10^{-4}$	$-2.281\,347 \times 10^{-2}$	$0(0)\rightarrow1(2v8,1v6,1v3,1v2)$
1.4836	$5.650\,680 \times 10^{-4}$	$2.377\,116 \times 10^{-2}$	$0(0)\rightarrow1(2v8,3v6,1v4,1v3)$

Continued on next page

Table S5: Table S5 – Continued from previous page

E_{BH} [eV]	Intensity [au]	FCF [au]	Transition
1.4995	$8.235\ 563 \times 10^{-4}$	$2.869\ 767 \times 10^{-2}$	$0(0) \rightarrow 1(5v8,1v2)$
1.5003	$5.398\ 049 \times 10^{-4}$	$2.323\ 370 \times 10^{-2}$	$0(0) \rightarrow 1(1v9,3v8,1v6,1v1)$
1.5081	$1.502\ 701 \times 10^{-3}$	$-3.876\ 469 \times 10^{-2}$	$0(0) \rightarrow 1(4v8,1v6,1v2)$
1.5088	$6.396\ 327 \times 10^{-4}$	$-2.529\ 096 \times 10^{-2}$	$0(0) \rightarrow 1(1v9,2v8,2v6,1v1)$
1.5163	$5.199\ 924 \times 10^{-4}$	$2.280\ 334 \times 10^{-2}$	$0(0) \rightarrow 1(4v8,3v6,1v4)$
1.5166	$1.457\ 512 \times 10^{-3}$	$3.817\ 737 \times 10^{-2}$	$0(0) \rightarrow 1(3v8,2v6,1v2)$
1.5174	$5.131\ 045 \times 10^{-4}$	$2.265\ 181 \times 10^{-2}$	$0(0) \rightarrow 1(1v9,1v8,3v6,1v1)$
1.5251	$8.681\ 297 \times 10^{-4}$	$-2.946\ 404 \times 10^{-2}$	$0(0) \rightarrow 1(2v8,3v6,1v2)$
1.5540	$5.087\ 894 \times 10^{-4}$	$-2.255\ 636 \times 10^{-2}$	$0(0) \rightarrow 1(4v8,1v4,1v2)$
1.5625	$8.698\ 106 \times 10^{-4}$	$2.949\ 255 \times 10^{-2}$	$0(0) \rightarrow 1(3v8,1v6,1v4,1v2)$
1.5711	$7.024\ 421 \times 10^{-4}$	$-2.650\ 362 \times 10^{-2}$	$0(0) \rightarrow 1(2v8,2v6,1v4,1v2)$
1.5840	$5.057\ 134 \times 10^{-4}$	$-2.248\ 807 \times 10^{-2}$	$0(0) \rightarrow 1(3v8,1v6,1v3,1v2)$
1.6167	$8.269\ 810 \times 10^{-4}$	$-2.875\ 728 \times 10^{-2}$	$0(0) \rightarrow 1(5v8,1v6,1v2)$
1.6252	$9.346\ 853 \times 10^{-4}$	$3.057\ 262 \times 10^{-2}$	$0(0) \rightarrow 1(4v8,2v6,1v2)$
1.6338	$7.154\ 857 \times 10^{-4}$	$-2.674\ 856 \times 10^{-2}$	$0(0) \rightarrow 1(3v8,3v6,1v2)$
1.6712	$5.656\ 530 \times 10^{-4}$	$2.378\ 346 \times 10^{-2}$	$0(0) \rightarrow 1(4v8,1v6,1v4,1v2)$
1.6797	$5.908\ 233 \times 10^{-4}$	$-2.430\ 686 \times 10^{-2}$	$0(0) \rightarrow 1(3v8,2v6,1v4,1v2)$

Table S6: ezSpectrum 3.0 simulations from CCSD(T)/A' VQZ geometries, harmonic frequencies and normal mode vectors. Data pertain to application of the Parallel Mode formalism. Simulation temperature of 10 K, intensity threshold of 1.0×10^{-3} au, maximum number of quanta in excited state $v = 10$.

E_{BH} [eV]	Intensity [au]	FCF [au]	Transition
0.5670	$2.631\ 643 \times 10^{-2}$	$1.622\ 234 \times 10^{-1}$	$0(0) \rightarrow 1(0)$
0.6330	$5.001\ 912 \times 10^{-3}$	$7.072\ 420 \times 10^{-2}$	$0(0) \rightarrow 1(1v7)$
0.6478	$7.771\ 837 \times 10^{-4}$	$2.787\ 802 \times 10^{-2}$	$0(0) \rightarrow 1(1v9)$
0.6756	$2.577\ 728 \times 10^{-2}$	$1.605\ 530 \times 10^{-1}$	$0(0) \rightarrow 1(1v8)$
0.6842	$2.997\ 164 \times 10^{-2}$	$-1.731\ 232 \times 10^{-1}$	$0(0) \rightarrow 1(1v6)$
0.6989	$8.608\ 812 \times 10^{-4}$	$2.934\ 078 \times 10^{-2}$	$0(0) \rightarrow 1(2v7)$
0.7206	$3.381\ 422 \times 10^{-3}$	$5.814\ 999 \times 10^{-2}$	$0(0) \rightarrow 1(1v5)$
0.7285	$1.863\ 135 \times 10^{-3}$	$4.316\ 405 \times 10^{-2}$	$0(0) \rightarrow 1(2v9)$
0.7301	$1.095\ 256 \times 10^{-2}$	$-1.046\ 545 \times 10^{-1}$	$0(0) \rightarrow 1(1v4)$
0.7416	$4.899\ 438 \times 10^{-3}$	$6.999\ 598 \times 10^{-2}$	$0(0) \rightarrow 1(1v7,1v8)$
0.7501	$5.696\ 651 \times 10^{-3}$	$-7.547\ 616 \times 10^{-2}$	$0(0) \rightarrow 1(1v7,1v6)$
0.7516	$4.662\ 671 \times 10^{-3}$	$6.828\ 376 \times 10^{-2}$	$0(0) \rightarrow 1(1v3)$
0.7564	$7.612\ 615 \times 10^{-4}$	$2.759\ 097 \times 10^{-2}$	$0(0) \rightarrow 1(1v9,1v8)$
0.7649	$8.851\ 304 \times 10^{-4}$	$-2.975\ 114 \times 10^{-2}$	$0(0) \rightarrow 1(1v9,1v6)$
0.7843	$1.787\ 438 \times 10^{-4}$	$1.336\ 951 \times 10^{-1}$	$0(0) \rightarrow 1(2v8)$
0.7866	$6.427\ 003 \times 10^{-2}$	$2.535\ 153 \times 10^{-2}$	$0(0) \rightarrow 1(1v7,1v5)$
0.7928	$2.935\ 760 \times 10^{-2}$	$-1.713\ 406 \times 10^{-1}$	$0(0) \rightarrow 1(1v8,1v6)$
0.7961	$2.081\ 732 \times 10^{-3}$	$-4.562\ 600 \times 10^{-2}$	$0(0) \rightarrow 1(1v7,1v4)$
0.8014	$2.013\ 154 \times 10^{-2}$	$1.418\ 857 \times 10^{-1}$	$0(0) \rightarrow 1(2v6)$
0.8076	$8.432\ 443 \times 10^{-4}$	$2.903\ 867 \times 10^{-2}$	$0(0) \rightarrow 1(2v7,1v8)$

Continued on next page

Table S6: Table S6 – Continued from previous page

E_{BH} [eV]	Intensity [au]	FCF [au]	Transition
0.8161	$9.804\,530 \times 10^{-4}$	$-3.131\,219 \times 10^{-2}$	$0(0) \rightarrow 1(2v7,1v6)$
0.8176	$8.862\,250 \times 10^{-4}$	$2.976\,953 \times 10^{-2}$	$0(0) \rightarrow 1(1v7,1v3)$
0.8292	$3.312\,146 \times 10^{-3}$	$5.755\,125 \times 10^{-2}$	$0(0) \rightarrow 1(1v8,1v5)$
0.8372	$1.824\,965 \times 10^{-3}$	$4.271\,960 \times 10^{-2}$	$0(0) \rightarrow 1(2v9,1v8)$
0.8378	$3.851\,083 \times 10^{-3}$	$-6.205\,709 \times 10^{-2}$	$0(0) \rightarrow 1(1v6,1v5)$
0.8388	$1.072\,817 \times 10^{-2}$	$-1.035\,769 \times 10^{-1}$	$0(0) \rightarrow 1(1v8,1v4)$
0.8457	$2.121\,914 \times 10^{-3}$	$-4.606\,424 \times 10^{-2}$	$0(0) \rightarrow 1(2v9,1v6)$
0.8473	$1.247\,381 \times 10^{-2}$	$1.116\,862 \times 10^{-1}$	$0(0) \rightarrow 1(1v6,1v4)$
0.8502	$3.397\,348 \times 10^{-3}$	$5.828\,678 \times 10^{-2}$	$0(0) \rightarrow 1(1v7,2v8)$
0.8588	$5.579\,943 \times 10^{-3}$	$-7.469\,902 \times 10^{-2}$	$0(0) \rightarrow 1(1v7,1v8,1v6)$
0.8603	$4.567\,147 \times 10^{-3}$	$6.758\,067 \times 10^{-2}$	$0(0) \rightarrow 1(1v8,1v3)$
0.8651	$5.278\,709 \times 10^{-4}$	$2.297\,544 \times 10^{-2}$	$0(0) \rightarrow 1(1v9,2v8)$
0.8673	$3.826\,363 \times 10^{-3}$	$6.185\,761 \times 10^{-2}$	$0(0) \rightarrow 1(1v7,2v6)$
0.8688	$5.310\,291 \times 10^{-3}$	$-7.287\,175 \times 10^{-2}$	$0(0) \rightarrow 1(1v6,1v3)$
0.8736	$8.669\,966 \times 10^{-4}$	$-2.944\,481 \times 10^{-2}$	$0(0) \rightarrow 1(1v9,1v8,1v6)$
0.8821	$5.945\,301 \times 10^{-4}$	$2.438\,299 \times 10^{-2}$	$0(0) \rightarrow 1(1v9,2v6)$
0.8837	$1.407\,304 \times 10^{-3}$	$-3.751\,406 \times 10^{-2}$	$0(0) \rightarrow 1(1v5,1v4)$
0.8916	$7.754\,129 \times 10^{-4}$	$-2.784\,624 \times 10^{-2}$	$0(0) \rightarrow 1(2v9,1v4)$
0.8929	$1.015\,601 \times 10^{-2}$	$1.007\,770 \times 10^{-1}$	$0(0) \rightarrow 1(3v8)$
0.8933	$2.558\,786 \times 10^{-3}$	$5.058\,445 \times 10^{-2}$	$0(0) \rightarrow 1(2v4)$
0.8952	$6.295\,332 \times 10^{-4}$	$2.509\,050 \times 10^{-2}$	$0(0) \rightarrow 1(1v7,1v8,1v5)$
0.9015	$2.035\,703 \times 10^{-2}$	$-1.426\,781 \times 10^{-1}$	$0(0) \rightarrow 1(2v8,1v6)$
0.9037	$7.319\,679 \times 10^{-4}$	$-2.705\,491 \times 10^{-2}$	$0(0) \rightarrow 1(1v7,1v6,1v5)$
0.9047	$2.039\,083 \times 10^{-3}$	$-4.515\,621 \times 10^{-2}$	$0(0) \rightarrow 1(1v7,1v8,1v4)$
0.9052	$5.991\,109 \times 10^{-4}$	$2.447\,674 \times 10^{-2}$	$0(0) \rightarrow 1(1v5,1v3)$
0.9100	$1.971\,910 \times 10^{-2}$	$1.404\,247 \times 10^{-1}$	$0(0) \rightarrow 1(1v8,2v6)$
0.9133	$2.370\,873 \times 10^{-3}$	$4.869\,161 \times 10^{-2}$	$0(0) \rightarrow 1(1v7,1v6,1v4)$
0.9148	$1.940\,544 \times 10^{-3}$	$-4.405\,161 \times 10^{-2}$	$0(0) \rightarrow 1(1v4,1v3)$
0.9162	$5.847\,190 \times 10^{-4}$	$2.418\,096 \times 10^{-2}$	$0(0) \rightarrow 1(2v7,2v8)$
0.9186	$1.025\,713 \times 10^{-2}$	$-1.012\,775 \times 10^{-1}$	$0(0) \rightarrow 1(3v6)$
0.9248	$9.603\,663 \times 10^{-4}$	$-3.098\,978 \times 10^{-2}$	$0(0) \rightarrow 1(2v7,1v8,1v6)$
0.9262	$8.680\,688 \times 10^{-4}$	$2.946\,301 \times 10^{-2}$	$0(0) \rightarrow 1(1v7,1v8,1v3)$
0.9333	$6.585\,570 \times 10^{-4}$	$2.566\,237 \times 10^{-2}$	$0(0) \rightarrow 1(2v7,2v6)$
0.9348	$1.009\,317 \times 10^{-3}$	$-3.176\,975 \times 10^{-2}$	$0(0) \rightarrow 1(1v7,1v6,1v3)$
0.9363	$5.260\,983 \times 10^{-4}$	$2.293\,683 \times 10^{-2}$	$0(0) \rightarrow 1(2v3)$
0.9379	$2.296\,695 \times 10^{-3}$	$4.792\,385 \times 10^{-2}$	$0(0) \rightarrow 1(2v8,1v5)$
0.9458	$1.265\,460 \times 10^{-3}$	$3.557\,330 \times 10^{-2}$	$0(0) \rightarrow 1(2v9,2v8)$
0.9464	$3.772\,185 \times 10^{-3}$	$-6.141\,812 \times 10^{-2}$	$0(0) \rightarrow 1(1v8,1v6,1v5)$
0.9474	$7.439\,087 \times 10^{-3}$	$-8.625\,014 \times 10^{-2}$	$0(0) \rightarrow 1(2v8,1v4)$
0.9544	$2.078\,442 \times 10^{-3}$	$-4.558\,994 \times 10^{-2}$	$0(0) \rightarrow 1(2v9,1v8,1v6)$
0.9550	$2.586\,720 \times 10^{-3}$	$5.085\,981 \times 10^{-2}$	$0(0) \rightarrow 1(2v6,1v5)$
0.9560	$1.221\,826 \times 10^{-2}$	$1.105\,362 \times 10^{-1}$	$0(0) \rightarrow 1(1v8,1v6,1v4)$
0.9563	$2.390\,178 \times 10^{-3}$	$4.888\,945 \times 10^{-2}$	$0(0) \rightarrow 1(1v2)$
0.9589	$1.930\,333 \times 10^{-3}$	$4.393\,555 \times 10^{-2}$	$0(0) \rightarrow 1(1v7,3v8)$
0.9629	$1.425\,261 \times 10^{-3}$	$3.775\,263 \times 10^{-2}$	$0(0) \rightarrow 1(2v9,2v6)$
0.9645	$8.378\,490 \times 10^{-3}$	$-9.153\,409 \times 10^{-2}$	$0(0) \rightarrow 1(2v6,1v4)$
0.9674	$3.869\,222 \times 10^{-3}$	$-6.220\,307 \times 10^{-2}$	$0(0) \rightarrow 1(1v7,2v8,1v6)$
0.9689	$3.166\,933 \times 10^{-3}$	$5.627\,551 \times 10^{-2}$	$0(0) \rightarrow 1(2v8,1v3)$
0.9760	$3.747\,972 \times 10^{-3}$	$6.122\,068 \times 10^{-2}$	$0(0) \rightarrow 1(1v7,1v8,2v6)$
0.9775	$5.201\,499 \times 10^{-3}$	$-7.212\,142 \times 10^{-2}$	$0(0) \rightarrow 1(1v8,1v6,1v3)$
0.9822	$6.011\,893 \times 10^{-4}$	$-2.451\,916 \times 10^{-2}$	$0(0) \rightarrow 1(1v9,2v8,1v6)$

Continued on next page

Table S6: Table S6 – Continued from previous page

E_{BH} [eV]	Intensity [au]	FCF [au]	Transition
0.9845	$1.949\,553 \times 10^{-3}$	$-4.415\,374 \times 10^{-2}$	$0(0) \rightarrow 1(1v7,3v6)$
0.9860	$3.566\,851 \times 10^{-3}$	$5.972\,312 \times 10^{-2}$	$0(0) \rightarrow 1(2v6,1v3)$
0.9908	$5.823\,499 \times 10^{-4}$	$2.413\,193 \times 10^{-2}$	$0(0) \rightarrow 1(1v9,1v8,2v6)$
0.9924	$1.378\,473 \times 10^{-3}$	$-3.712\,779 \times 10^{-2}$	$0(0) \rightarrow 1(1v8,1v5,1v4)$
1.0003	$7.595\,269 \times 10^{-4}$	$-2.755\,952 \times 10^{-2}$	$0(0) \rightarrow 1(2v9,1v8,1v4)$
1.0009	$1.602\,771 \times 10^{-3}$	$4.003\,463 \times 10^{-2}$	$0(0) \rightarrow 1(1v6,1v5,1v4)$
1.0016	$5.098\,724 \times 10^{-3}$	$7.140\,535 \times 10^{-2}$	$0(0) \rightarrow 1(4v8)$
1.0019	$2.506\,364 \times 10^{-3}$	$5.006\,360 \times 10^{-2}$	$0(0) \rightarrow 1(1v8,2v4)$
1.0088	$8.831\,135 \times 10^{-4}$	$2.971\,723 \times 10^{-2}$	$0(0) \rightarrow 1(2v9,1v6,1v4)$
1.0101	$1.156\,662 \times 10^{-2}$	$-1.075\,482 \times 10^{-1}$	$0(0) \rightarrow 1(3v8,1v6)$
1.0104	$2.914\,188 \times 10^{-3}$	$-5.398\,322 \times 10^{-2}$	$0(0) \rightarrow 1(1v6,2v4)$
1.0124	$7.169\,720 \times 10^{-4}$	$-2.677\,633 \times 10^{-2}$	$0(0) \rightarrow 1(1v7,1v8,1v6,1v5)$
1.0134	$1.413\,933 \times 10^{-3}$	$-3.760\,230 \times 10^{-2}$	$0(0) \rightarrow 1(1v7,2v8,1v4)$
1.0139	$5.868\,369 \times 10^{-4}$	$2.422\,472 \times 10^{-2}$	$0(0) \rightarrow 1(1v8,1v5,1v3)$
1.0187	$1.367\,354 \times 10^{-2}$	$1.169\,339 \times 10^{-1}$	$0(0) \rightarrow 1(2v8,2v6)$
1.0219	$2.322\,301 \times 10^{-3}$	$4.819\,026 \times 10^{-2}$	$0(0) \rightarrow 1(1v7,1v8,1v6,1v4)$
1.0224	$6.823\,242 \times 10^{-4}$	$-2.612\,134 \times 10^{-2}$	$0(0) \rightarrow 1(1v6,1v5,1v3)$
1.0234	$1.900\,788 \times 10^{-3}$	$-4.359\,803 \times 10^{-2}$	$0(0) \rightarrow 1(1v8,1v4,1v3)$
1.0272	$1.004\,699 \times 10^{-2}$	$-1.002\,347 \times 10^{-1}$	$0(0) \rightarrow 1(1v8,3v6)$
1.0305	$1.592\,484 \times 10^{-3}$	$-3.990\,593 \times 10^{-2}$	$0(0) \rightarrow 1(1v7,2v6,1v4)$
1.0319	$2.210\,075 \times 10^{-3}$	$4.701\,144 \times 10^{-2}$	$0(0) \rightarrow 1(1v6,1v4,1v3)$
1.0334	$6.659\,333 \times 10^{-4}$	$-2.580\,568 \times 10^{-2}$	$0(0) \rightarrow 1(2v7,2v8,1v6)$
1.0349	$6.019\,328 \times 10^{-4}$	$2.453\,432 \times 10^{-2}$	$0(0) \rightarrow 1(1v7,2v8,1v3)$
1.0357	$4.367\,313 \times 10^{-3}$	$6.608\,565 \times 10^{-2}$	$0(0) \rightarrow 1(4v6)$
1.0419	$6.450\,651 \times 10^{-4}$	$2.539\,813 \times 10^{-2}$	$0(0) \rightarrow 1(2v7,1v8,2v6)$
1.0434	$9.886\,389 \times 10^{-4}$	$-3.144\,263 \times 10^{-2}$	$0(0) \rightarrow 1(1v7,1v8,1v6,1v3)$
1.0449	$5.153\,200 \times 10^{-4}$	$2.270\,066 \times 10^{-2}$	$0(0) \rightarrow 1(1v8,2v3)$
1.0465	$1.304\,955 \times 10^{-3}$	$3.612\,415 \times 10^{-2}$	$0(0) \rightarrow 1(3v8,1v5)$
1.0520	$6.779\,445 \times 10^{-4}$	$2.603\,737 \times 10^{-2}$	$0(0) \rightarrow 1(1v7,2v6,1v3)$
1.0534	$5.991\,705 \times 10^{-4}$	$-2.447\,796 \times 10^{-2}$	$0(0) \rightarrow 1(1v6,2v3)$
1.0545	$7.190\,189 \times 10^{-4}$	$2.681\,453 \times 10^{-2}$	$0(0) \rightarrow 1(2v9,3v8)$
1.0551	$2.615\,694 \times 10^{-3}$	$-5.114\,385 \times 10^{-2}$	$0(0) \rightarrow 1(2v8,1v6,1v5)$
1.0561	$4.226\,800 \times 10^{-3}$	$-6.501\,384 \times 10^{-2}$	$0(0) \rightarrow 1(3v8,1v4)$
1.0630	$1.441\,225 \times 10^{-3}$	$-3.796\,347 \times 10^{-2}$	$0(0) \rightarrow 1(2v9,2v8,1v6)$
1.0636	$2.533\,726 \times 10^{-3}$	$5.033\,613 \times 10^{-2}$	$0(0) \rightarrow 1(1v8,2v6,1v5)$
1.0646	$8.472\,336 \times 10^{-3}$	$9.204\,529 \times 10^{-2}$	$0(0) \rightarrow 1(2v8,1v6,1v4)$
1.0649	$2.341\,210 \times 10^{-3}$	$4.838\,606 \times 10^{-2}$	$0(0) \rightarrow 1(1v8,1v2)$
1.0675	$9.691\,047 \times 10^{-4}$	$3.113\,045 \times 10^{-2}$	$0(0) \rightarrow 1(1v7,4v8)$
1.0715	$1.396\,062 \times 10^{-3}$	$3.736\,391 \times 10^{-2}$	$0(0) \rightarrow 1(2v9,1v8,2v6)$
1.0722	$1.317\,948 \times 10^{-3}$	$-3.630\,355 \times 10^{-2}$	$0(0) \rightarrow 1(3v6,1v5)$
1.0731	$8.206\,839 \times 10^{-3}$	$-9.059\,161 \times 10^{-2}$	$0(0) \rightarrow 1(1v8,2v6,1v4)$
1.0735	$2.722\,161 \times 10^{-3}$	$-5.217\,433 \times 10^{-2}$	$0(0) \rightarrow 1(1v6,1v2)$
1.0761	$2.198\,445 \times 10^{-3}$	$-4.688\,758 \times 10^{-2}$	$0(0) \rightarrow 1(1v7,3v8,1v6)$
1.0764	$5.538\,940 \times 10^{-4}$	$-2.353\,495 \times 10^{-2}$	$0(0) \rightarrow 1(1v7,1v6,2v4)$
1.0776	$1.799\,413 \times 10^{-3}$	$4.241\,949 \times 10^{-2}$	$0(0) \rightarrow 1(3v8,1v3)$
1.0801	$7.261\,782 \times 10^{-4}$	$-2.694\,769 \times 10^{-2}$	$0(0) \rightarrow 1(2v9,3v6)$
1.0817	$4.268\,886 \times 10^{-3}$	$6.533\,671 \times 10^{-2}$	$0(0) \rightarrow 1(3v6,1v4)$
1.0846	$2.598\,904 \times 10^{-3}$	$5.097\,944 \times 10^{-2}$	$0(0) \rightarrow 1(1v7,2v8,2v6)$
1.0861	$3.606\,802 \times 10^{-3}$	$-6.005\,666 \times 10^{-2}$	$0(0) \rightarrow 1(2v8,1v6,1v3)$
1.0932	$1.909\,612 \times 10^{-3}$	$-4.369\,911 \times 10^{-2}$	$0(0) \rightarrow 1(1v7,1v8,3v6)$
1.0946	$3.493\,776 \times 10^{-3}$	$5.910\,818 \times 10^{-2}$	$0(0) \rightarrow 1(1v8,2v6,1v3)$

Continued on next page

Table S6: Table S6 – Continued from previous page

E_{BH} [eV]	Intensity [au]	FCF [au]	Transition
1.1010	$9.558\,551 \times 10^{-4}$	$-3.091\,691 \times 10^{-2}$	$0(0) \rightarrow 1(2v8,1v5,1v4)$
1.1017	$8.300\,868 \times 10^{-4}$	$2.881\,123 \times 10^{-2}$	$0(0) \rightarrow 1(1v7,4v6)$
1.1032	$1.817\,330 \times 10^{-3}$	$-4.263\,015 \times 10^{-2}$	$0(0) \rightarrow 1(3v6,1v3)$
1.1089	$5.266\,681 \times 10^{-4}$	$-2.294\,925 \times 10^{-2}$	$0(0) \rightarrow 1(2v9,2v8,1v4)$
1.1096	$1.569\,935 \times 10^{-3}$	$3.962\,241 \times 10^{-2}$	$0(0) \rightarrow 1(1v8,1v6,1v5,1v4)$
1.1102	$2.339\,679 \times 10^{-3}$	$4.837\,023 \times 10^{-2}$	$0(0) \rightarrow 1(5v8)$
1.1105	$1.737\,953 \times 10^{-3}$	$4.168\,876 \times 10^{-2}$	$0(0) \rightarrow 1(2v8,2v4)$
1.1175	$8.650\,211 \times 10^{-4}$	$2.941\,124 \times 10^{-2}$	$0(0) \rightarrow 1(2v9,1v8,1v6,1v4)$
1.1181	$1.076\,560 \times 10^{-3}$	$-3.281\,097 \times 10^{-2}$	$0(0) \rightarrow 1(2v6,1v5,1v4)$
1.1188	$5.806\,910 \times 10^{-3}$	$-7.620\,308 \times 10^{-2}$	$0(0) \rightarrow 1(4v8,1v6)$
1.1191	$2.854\,484 \times 10^{-3}$	$-5.342\,738 \times 10^{-2}$	$0(0) \rightarrow 1(1v8,1v6,2v4)$
1.1194	$9.947\,616 \times 10^{-4}$	$-3.153\,984 \times 10^{-2}$	$0(0) \rightarrow 1(1v4,1v2)$
1.1220	$8.033\,797 \times 10^{-4}$	$-2.834\,395 \times 10^{-2}$	$0(0) \rightarrow 1(1v7,3v8,1v4)$
1.1260	$5.931\,754 \times 10^{-4}$	$-2.435\,519 \times 10^{-2}$	$0(0) \rightarrow 1(2v9,2v6,1v4)$
1.1273	$7.769\,142 \times 10^{-3}$	$8.814\,274 \times 10^{-2}$	$0(0) \rightarrow 1(3v8,2v6)$
1.1276	$1.957\,420 \times 10^{-3}$	$4.424\,274 \times 10^{-2}$	$0(0) \rightarrow 1(2v6,2v4)$
1.1306	$1.610\,321 \times 10^{-3}$	$4.012\,880 \times 10^{-2}$	$0(0) \rightarrow 1(1v7,2v8,1v6,1v4)$
1.1311	$6.683\,453 \times 10^{-4}$	$-2.585\,238 \times 10^{-2}$	$0(0) \rightarrow 1(1v8,1v6,1v5,1v3)$
1.1320	$1.318\,037 \times 10^{-3}$	$-3.630\,478 \times 10^{-2}$	$0(0) \rightarrow 1(2v8,1v4,1v3)$
1.1358	$6.966\,744 \times 10^{-3}$	$-8.346\,702 \times 10^{-2}$	$0(0) \rightarrow 1(2v8,3v6)$
1.1391	$1.559\,858 \times 10^{-3}$	$-3.949\,504 \times 10^{-2}$	$0(0) \rightarrow 1(1v7,1v8,2v6,1v4)$
1.1394	$5.173\,959 \times 10^{-4}$	$-2.274\,634 \times 10^{-2}$	$0(0) \rightarrow 1(1v7,1v6,1v2)$
1.1406	$2.164\,797 \times 10^{-3}$	$4.652\,738 \times 10^{-2}$	$0(0) \rightarrow 1(1v8,1v6,1v4,1v3)$
1.1444	$4.277\,839 \times 10^{-3}$	$6.540\,519 \times 10^{-2}$	$0(0) \rightarrow 1(1v8,4v6)$
1.1476	$8.113\,790 \times 10^{-4}$	$2.848\,472 \times 10^{-2}$	$0(0) \rightarrow 1(1v7,3v6,1v4)$
1.1491	$1.484\,478 \times 10^{-3}$	$-3.852\,892 \times 10^{-2}$	$0(0) \rightarrow 1(2v6,1v4,1v3)$
1.1521	$6.855\,380 \times 10^{-4}$	$-2.618\,278 \times 10^{-2}$	$0(0) \rightarrow 1(1v7,2v8,1v6,1v3)$
1.1529	$1.633\,730 \times 10^{-3}$	$-4.041\,943 \times 10^{-2}$	$0(0) \rightarrow 1(5v6)$
1.1552	$6.551\,398 \times 10^{-4}$	$2.559\,570 \times 10^{-2}$	$0(0) \rightarrow 1(4v8,1v5)$
1.1606	$6.640\,553 \times 10^{-4}$	$2.576\,927 \times 10^{-2}$	$0(0) \rightarrow 1(1v7,1v8,2v6,1v3)$
1.1621	$5.868\,952 \times 10^{-4}$	$-2.422\,592 \times 10^{-2}$	$0(0) \rightarrow 1(1v8,1v6,2v3)$
1.1637	$1.486\,206 \times 10^{-3}$	$-3.855\,134 \times 10^{-2}$	$0(0) \rightarrow 1(3v8,1v6,1v5)$
1.1647	$2.122\,024 \times 10^{-3}$	$-4.606\,543 \times 10^{-2}$	$0(0) \rightarrow 1(4v8,1v4)$
1.1716	$8.188\,868 \times 10^{-4}$	$-2.861\,620 \times 10^{-2}$	$0(0) \rightarrow 1(2v9,3v8,1v6)$
1.1723	$1.756\,926 \times 10^{-3}$	$4.191\,570 \times 10^{-2}$	$0(0) \rightarrow 1(2v8,2v6,1v5)$
1.1732	$4.813\,880 \times 10^{-3}$	$6.938\,213 \times 10^{-2}$	$0(0) \rightarrow 1(3v8,1v6,1v4)$
1.1736	$5.003\,111 \times 10^{-4}$	$2.236\,763 \times 10^{-2}$	$0(0) \rightarrow 1(1v6,3v4)$
1.1736	$1.623\,433 \times 10^{-3}$	$4.029\,184 \times 10^{-2}$	$0(0) \rightarrow 1(2v8,1v2)$
1.1802	$9.680\,514 \times 10^{-4}$	$3.111\,352 \times 10^{-2}$	$0(0) \rightarrow 1(2v9,2v8,2v6)$
1.1808	$1.290\,947 \times 10^{-3}$	$-3.592\,975 \times 10^{-2}$	$0(0) \rightarrow 1(1v8,3v6,1v5)$
1.1818	$5.690\,753 \times 10^{-3}$	$-7.543\,708 \times 10^{-2}$	$0(0) \rightarrow 1(2v8,2v6,1v4)$
1.1821	$2.666\,392 \times 10^{-3}$	$-5.163\,712 \times 10^{-2}$	$0(0) \rightarrow 1(1v8,1v6,1v2)$
1.1847	$1.103\,708 \times 10^{-3}$	$-3.322\,210 \times 10^{-2}$	$0(0) \rightarrow 1(1v7,4v8,1v6)$
1.1850	$5.425\,463 \times 10^{-4}$	$-2.329\,262 \times 10^{-2}$	$0(0) \rightarrow 1(1v7,1v8,1v6,2v4)$
1.1862	$9.033\,779 \times 10^{-4}$	$3.005\,625 \times 10^{-2}$	$0(0) \rightarrow 1(4v8,1v3)$
1.1887	$7.113\,009 \times 10^{-4}$	$-2.667\,023 \times 10^{-2}$	$0(0) \rightarrow 1(2v9,1v8,3v6)$
1.1893	$5.611\,601 \times 10^{-4}$	$2.368\,882 \times 10^{-2}$	$0(0) \rightarrow 1(4v6,1v5)$
1.1903	$4.181\,429 \times 10^{-3}$	$6.466\,397 \times 10^{-2}$	$0(0) \rightarrow 1(1v8,3v6,1v4)$
1.1907	$1.828\,439 \times 10^{-3}$	$4.276\,025 \times 10^{-2}$	$0(0) \rightarrow 1(2v6,1v2)$
1.1933	$1.476\,666 \times 10^{-3}$	$3.842\,741 \times 10^{-2}$	$0(0) \rightarrow 1(1v7,3v8,2v6)$
1.1947	$2.049\,342 \times 10^{-3}$	$-4.526\,966 \times 10^{-2}$	$0(0) \rightarrow 1(3v8,1v6,1v3)$

Continued on next page

Table S6: Table S6 – Continued from previous page

E_{BH} [eV]	Intensity [au]	FCF [au]	Transition
1.1951	$5.163\,277 \times 10^{-4}$	$-2.272\,285 \times 10^{-2}$	$0(0) \rightarrow 1(1v6,2v4,1v3)$
1.1989	$1.817\,620 \times 10^{-3}$	$-4.263\,355 \times 10^{-2}$	$0(0) \rightarrow 1(4v6,1v4)$
1.2018	$1.324\,156 \times 10^{-3}$	$-3.638\,895 \times 10^{-2}$	$0(0) \rightarrow 1(1v7,2v8,3v6)$
1.2033	$2.422\,640 \times 10^{-3}$	$4.922\,032 \times 10^{-2}$	$0(0) \rightarrow 1(2v8,2v6,1v3)$
1.2097	$5.431\,054 \times 10^{-4}$	$-2.330\,462 \times 10^{-2}$	$0(0) \rightarrow 1(3v8,1v5,1v4)$
1.2103	$8.130\,807 \times 10^{-4}$	$2.851\,457 \times 10^{-2}$	$0(0) \rightarrow 1(1v7,1v8,4v6)$
1.2118	$1.780\,098 \times 10^{-3}$	$-4.219\,121 \times 10^{-2}$	$0(0) \rightarrow 1(1v8,3v6,1v3)$
1.2182	$1.088\,618 \times 10^{-3}$	$3.299\,421 \times 10^{-2}$	$0(0) \rightarrow 1(2v8,1v6,1v5,1v4)$
1.2189	$1.002\,857 \times 10^{-3}$	$3.166\,792 \times 10^{-2}$	$0(0) \rightarrow 1(6v8)$
1.2192	$9.874\,839 \times 10^{-4}$	$3.142\,426 \times 10^{-2}$	$0(0) \rightarrow 1(3v8,2v4)$
1.2204	$7.737\,884 \times 10^{-4}$	$2.781\,705 \times 10^{-2}$	$0(0) \rightarrow 1(4v6,1v3)$
1.2261	$5.998\,194 \times 10^{-4}$	$2.449\,121 \times 10^{-2}$	$0(0) \rightarrow 1(2v9,2v8,1v6,1v4)$
1.2267	$1.054\,504 \times 10^{-3}$	$-3.247\,313 \times 10^{-2}$	$0(0) \rightarrow 1(1v8,2v6,1v5,1v4)$
1.2274	$2.664\,648 \times 10^{-3}$	$-5.162\,023 \times 10^{-2}$	$0(0) \rightarrow 1(5v8,1v6)$
1.2277	$1.979\,345 \times 10^{-3}$	$-4.448\,983 \times 10^{-2}$	$0(0) \rightarrow 1(2v8,1v6,2v4)$
1.2281	$9.743\,818 \times 10^{-4}$	$-3.121\,509 \times 10^{-2}$	$0(0) \rightarrow 1(1v8,1v4,1v2)$
1.2347	$5.810\,230 \times 10^{-4}$	$-2.410\,442 \times 10^{-2}$	$0(0) \rightarrow 1(2v9,1v8,2v6,1v4)$
1.2353	$5.485\,131 \times 10^{-4}$	$2.342\,036 \times 10^{-2}$	$0(0) \rightarrow 1(3v6,1v5,1v4)$
1.2359	$3.900\,423 \times 10^{-3}$	$6.245\,336 \times 10^{-2}$	$0(0) \rightarrow 1(4v8,2v6)$
1.2363	$1.917\,319 \times 10^{-3}$	$4.378\,720 \times 10^{-2}$	$0(0) \rightarrow 1(1v8,2v6,2v4)$
1.2366	$1.132\,929 \times 10^{-3}$	$3.365\,901 \times 10^{-2}$	$0(0) \rightarrow 1(1v6,1v4,1v2)$
1.2392	$9.149\,648 \times 10^{-4}$	$3.024\,839 \times 10^{-2}$	$0(0) \rightarrow 1(1v7,3v8,1v6,1v4)$
1.2407	$7.488\,927 \times 10^{-4}$	$-2.736\,590 \times 10^{-2}$	$0(0) \rightarrow 1(3v8,1v4,1v3)$
1.2445	$3.958\,420 \times 10^{-3}$	$-6.291\,598 \times 10^{-2}$	$0(0) \rightarrow 1(3v8,3v6)$
1.2448	$9.973\,163 \times 10^{-4}$	$-3.158\,032 \times 10^{-2}$	$0(0) \rightarrow 1(3v6,2v4)$
1.2477	$1.081\,631 \times 10^{-3}$	$-3.288\,815 \times 10^{-2}$	$0(0) \rightarrow 1(1v7,2v8,2v6,1v4)$
1.2481	$5.067\,960 \times 10^{-4}$	$-2.251\,213 \times 10^{-2}$	$0(0) \rightarrow 1(1v7,1v8,1v6,1v2)$
1.2492	$1.501\,105 \times 10^{-3}$	$3.874\,410 \times 10^{-2}$	$0(0) \rightarrow 1(2v8,1v6,1v4,1v3)$
1.2530	$2.966\,322 \times 10^{-3}$	$5.446\,395 \times 10^{-2}$	$0(0) \rightarrow 1(2v8,4v6)$
1.2563	$7.947\,562 \times 10^{-4}$	$2.819\,142 \times 10^{-2}$	$0(0) \rightarrow 1(1v7,1v8,3v6,1v4)$
1.2578	$1.454\,065 \times 10^{-3}$	$-3.813\,221 \times 10^{-2}$	$0(0) \rightarrow 1(1v8,2v6,1v4,1v3)$
1.2616	$1.600\,260 \times 10^{-3}$	$-4.000\,325 \times 10^{-2}$	$0(0) \rightarrow 1(1v8,5v6)$
1.2663	$7.563\,495 \times 10^{-4}$	$2.750\,181 \times 10^{-2}$	$0(0) \rightarrow 1(3v6,1v4,1v3)$
1.2701	$5.533\,435 \times 10^{-4}$	$2.352\,325 \times 10^{-2}$	$0(0) \rightarrow 1(6v6)$
1.2724	$7.461\,351 \times 10^{-4}$	$-2.731\,547 \times 10^{-2}$	$0(0) \rightarrow 1(4v8,1v6,1v5)$
1.2733	$9.737\,446 \times 10^{-4}$	$-3.120\,488 \times 10^{-2}$	$0(0) \rightarrow 1(5v8,1v4)$
1.2809	$9.982\,642 \times 10^{-4}$	$3.159\,532 \times 10^{-2}$	$0(0) \rightarrow 1(3v8,2v6,1v5)$
1.2819	$2.416\,762 \times 10^{-3}$	$4.916\,057 \times 10^{-2}$	$0(0) \rightarrow 1(4v8,1v6,1v4)$
1.2822	$9.224\,149 \times 10^{-4}$	$3.037\,128 \times 10^{-2}$	$0(0) \rightarrow 1(3v8,1v2)$
1.2888	$5.500\,352 \times 10^{-4}$	$2.345\,283 \times 10^{-2}$	$0(0) \rightarrow 1(2v9,3v8,2v6)$
1.2894	$8.951\,633 \times 10^{-4}$	$-2.991\,928 \times 10^{-2}$	$0(0) \rightarrow 1(2v8,3v6,1v5)$
1.2904	$3.233\,418 \times 10^{-3}$	$-5.686\,315 \times 10^{-2}$	$0(0) \rightarrow 1(3v8,2v6,1v4)$
1.2908	$1.848\,919 \times 10^{-3}$	$-4.299\,905 \times 10^{-2}$	$0(0) \rightarrow 1(2v8,1v6,1v2)$
1.2934	$5.064\,645 \times 10^{-4}$	$-2.250\,477 \times 10^{-2}$	$0(0) \rightarrow 1(1v7,5v8,1v6)$
1.2980	$5.496\,635 \times 10^{-4}$	$2.344\,490 \times 10^{-2}$	$0(0) \rightarrow 1(1v8,4v6,1v5)$
1.2990	$2.899\,470 \times 10^{-3}$	$5.384\,672 \times 10^{-2}$	$0(0) \rightarrow 1(2v8,3v6,1v4)$
1.2993	$1.790\,979 \times 10^{-3}$	$4.231\,996 \times 10^{-2}$	$0(0) \rightarrow 1(1v8,2v6,1v2)$
1.3019	$7.413\,458 \times 10^{-4}$	$2.722\,767 \times 10^{-2}$	$0(0) \rightarrow 1(1v7,4v8,2v6)$
1.3034	$1.028\,852 \times 10^{-3}$	$-3.207\,573 \times 10^{-2}$	$0(0) \rightarrow 1(4v8,1v6,1v3)$
1.3037	$5.057\,496 \times 10^{-4}$	$-2.248\,888 \times 10^{-2}$	$0(0) \rightarrow 1(1v8,1v6,2v4,1v3)$
1.3075	$1.780\,382 \times 10^{-3}$	$-4.219\,457 \times 10^{-2}$	$0(0) \rightarrow 1(1v8,4v6,1v4)$

Continued on next page

Table S6: Table S6 – Continued from previous page

E_{BH} [eV]	Intensity [au]	FCF [au]	Transition
1.3078	$9.315\ 995 \times 10^{-4}$	$-3.052\ 211 \times 10^{-2}$	$0(0) \rightarrow 1(3v6,1v2)$
1.3105	$7.523\ 693 \times 10^{-4}$	$-2.742\ 935 \times 10^{-2}$	$0(0) \rightarrow 1(1v7,3v8,3v6)$
1.3119	$1.376\ 515 \times 10^{-3}$	$3.710\ 142 \times 10^{-2}$	$0(0) \rightarrow 1(3v8,2v6,1v3)$
1.3161	$6.799\ 376 \times 10^{-4}$	$2.607\ 561 \times 10^{-2}$	$0(0) \rightarrow 1(5v6,1v4)$
1.3190	$5.638\ 031 \times 10^{-4}$	$2.374\ 454 \times 10^{-2}$	$0(0) \rightarrow 1(1v7,2v8,4v6)$
1.3205	$1.234\ 348 \times 10^{-3}$	$-3.513\ 329 \times 10^{-2}$	$0(0) \rightarrow 1(2v8,3v6,1v3)$
1.3268	$6.185\ 398 \times 10^{-4}$	$2.487\ 046 \times 10^{-2}$	$0(0) \rightarrow 1(3v8,1v6,1v5,1v4)$
1.3290	$7.579\ 358 \times 10^{-4}$	$2.753\ 063 \times 10^{-2}$	$0(0) \rightarrow 1(1v8,4v6,1v3)$
1.3354	$7.312\ 101 \times 10^{-4}$	$-2.704\ 090 \times 10^{-2}$	$0(0) \rightarrow 1(2v8,2v6,1v5,1v4)$
1.3361	$1.142\ 149 \times 10^{-3}$	$-3.379\ 569 \times 10^{-2}$	$0(0) \rightarrow 1(6v8,1v6)$
1.3364	$1.124\ 640 \times 10^{-3}$	$-3.353\ 565 \times 10^{-2}$	$0(0) \rightarrow 1(3v8,1v6,2v4)$
1.3367	$6.756\ 519 \times 10^{-4}$	$-2.599\ 331 \times 10^{-2}$	$0(0) \rightarrow 1(2v8,1v4,1v2)$
1.3439	$5.372\ 757 \times 10^{-4}$	$2.317\ 921 \times 10^{-2}$	$0(0) \rightarrow 1(1v8,3v6,1v5,1v4)$
1.3446	$1.789\ 808 \times 10^{-3}$	$4.230\ 612 \times 10^{-2}$	$0(0) \rightarrow 1(5v8,2v6)$
1.3449	$1.329\ 499 \times 10^{-3}$	$3.646\ 230 \times 10^{-2}$	$0(0) \rightarrow 1(2v8,2v6,2v4)$
1.3452	$1.109\ 718 \times 10^{-3}$	$3.331\ 243 \times 10^{-2}$	$0(0) \rightarrow 1(1v8,1v6,1v4,1v2)$
1.3531	$1.987\ 287 \times 10^{-3}$	$-4.457\ 899 \times 10^{-2}$	$0(0) \rightarrow 1(4v8,3v6)$
1.3535	$9.768\ 842 \times 10^{-4}$	$-3.125\ 515 \times 10^{-2}$	$0(0) \rightarrow 1(1v8,3v6,2v4)$
1.3538	$7.609\ 728 \times 10^{-4}$	$-2.758\ 574 \times 10^{-2}$	$0(0) \rightarrow 1(2v6,1v4,1v2)$
1.3564	$6.145\ 695 \times 10^{-4}$	$-2.479\ 051 \times 10^{-2}$	$0(0) \rightarrow 1(1v7,3v8,2v6,1v4)$
1.3579	$8.529\ 099 \times 10^{-4}$	$2.920\ 462 \times 10^{-2}$	$0(0) \rightarrow 1(3v8,1v6,1v4,1v3)$
1.3617	$1.685\ 429 \times 10^{-3}$	$4.105\ 397 \times 10^{-2}$	$0(0) \rightarrow 1(3v8,4v6)$
1.3649	$5.510\ 966 \times 10^{-4}$	$2.347\ 545 \times 10^{-2}$	$0(0) \rightarrow 1(1v7,2v8,3v6,1v4)$
1.3664	$1.008\ 272 \times 10^{-3}$	$-3.175\ 330 \times 10^{-2}$	$0(0) \rightarrow 1(2v8,2v6,1v4,1v3)$
1.3702	$1.109\ 646 \times 10^{-3}$	$-3.331\ 134 \times 10^{-2}$	$0(0) \rightarrow 1(2v8,5v6)$
1.3750	$7.408\ 540 \times 10^{-4}$	$2.721\ 863 \times 10^{-2}$	$0(0) \rightarrow 1(1v8,3v6,1v4,1v3)$
1.3788	$5.420\ 071 \times 10^{-4}$	$2.328\ 105 \times 10^{-2}$	$0(0) \rightarrow 1(1v8,6v6)$
1.3896	$5.011\ 689 \times 10^{-4}$	$2.238\ 680 \times 10^{-2}$	$0(0) \rightarrow 1(4v8,2v6,1v5)$
1.3905	$1.108\ 992 \times 10^{-3}$	$3.330\ 154 \times 10^{-2}$	$0(0) \rightarrow 1(5v8,1v6,1v4)$
1.3981	$5.086\ 210 \times 10^{-4}$	$-2.255\ 263 \times 10^{-2}$	$0(0) \rightarrow 1(3v8,3v6,1v5)$
1.3991	$1.623\ 306 \times 10^{-3}$	$-4.029\ 027 \times 10^{-2}$	$0(0) \rightarrow 1(4v8,2v6,1v4)$
1.3994	$1.050\ 533 \times 10^{-3}$	$-3.241\ 193 \times 10^{-2}$	$0(0) \rightarrow 1(3v8,1v6,1v2)$
1.4076	$1.647\ 444 \times 10^{-3}$	$4.058\ 872 \times 10^{-2}$	$0(0) \rightarrow 1(3v8,3v6,1v4)$
1.4079	$1.241\ 894 \times 10^{-3}$	$3.524\ 051 \times 10^{-2}$	$0(0) \rightarrow 1(2v8,2v6,1v2)$
1.4162	$1.234\ 545 \times 10^{-3}$	$-3.513\ 610 \times 10^{-2}$	$0(0) \rightarrow 1(2v8,4v6,1v4)$
1.4165	$9.125\ 137 \times 10^{-4}$	$-3.020\ 784 \times 10^{-2}$	$0(0) \rightarrow 1(1v8,3v6,1v2)$
1.4206	$6.910\ 661 \times 10^{-4}$	$2.628\ 814 \times 10^{-2}$	$0(0) \rightarrow 1(4v8,2v6,1v3)$
1.4247	$6.660\ 076 \times 10^{-4}$	$2.580\ 712 \times 10^{-2}$	$0(0) \rightarrow 1(1v8,5v6,1v4)$
1.4291	$7.013\ 419 \times 10^{-4}$	$-2.648\ 286 \times 10^{-2}$	$0(0) \rightarrow 1(3v8,3v6,1v3)$
1.4377	$5.255\ 648 \times 10^{-4}$	$2.292\ 520 \times 10^{-2}$	$0(0) \rightarrow 1(2v8,4v6,1v3)$
1.4450	$5.646\ 147 \times 10^{-4}$	$-2.376\ 162 \times 10^{-2}$	$0(0) \rightarrow 1(4v8,1v6,2v4)$
1.4532	$7.671\ 659 \times 10^{-4}$	$2.769\ 776 \times 10^{-2}$	$0(0) \rightarrow 1(6v8,2v6)$
1.4536	$7.554\ 055 \times 10^{-4}$	$2.748\ 464 \times 10^{-2}$	$0(0) \rightarrow 1(3v8,2v6,2v4)$
1.4539	$7.694\ 963 \times 10^{-4}$	$2.773\ 980 \times 10^{-2}$	$0(0) \rightarrow 1(2v8,1v6,1v4,1v2)$
1.4618	$9.119\ 169 \times 10^{-4}$	$-3.019\ 796 \times 10^{-2}$	$0(0) \rightarrow 1(5v8,3v6)$
1.4621	$6.773\ 871 \times 10^{-4}$	$-2.602\ 666 \times 10^{-2}$	$0(0) \rightarrow 1(2v8,3v6,2v4)$
1.4624	$7.453\ 827 \times 10^{-4}$	$-2.730\ 170 \times 10^{-2}$	$0(0) \rightarrow 1(1v8,2v6,1v4,1v2)$
1.4703	$8.461\ 531 \times 10^{-4}$	$2.908\ 871 \times 10^{-2}$	$0(0) \rightarrow 1(4v8,4v6)$
1.4751	$5.728\ 880 \times 10^{-4}$	$-2.393\ 508 \times 10^{-2}$	$0(0) \rightarrow 1(3v8,2v6,1v4,1v3)$
1.4789	$6.304\ 873 \times 10^{-4}$	$-2.510\ 951 \times 10^{-2}$	$0(0) \rightarrow 1(3v8,5v6)$
1.4836	$5.137\ 200 \times 10^{-4}$	$2.266\ 539 \times 10^{-2}$	$0(0) \rightarrow 1(2v8,3v6,1v4,1v3)$

Continued on next page

Table S6: Table S6 – Continued from previous page

E_{BH} [eV]	Intensity [au]	FCF [au]	Transition
1.5077	$7.448\ 952 \times 10^{-4}$	$-2.729\ 277 \times 10^{-2}$	$0(0) \rightarrow 1(5v8,2v6,1v4)$
1.5081	$5.274\ 101 \times 10^{-4}$	$-2.296\ 541 \times 10^{-2}$	$0(0) \rightarrow 1(4v8,1v6,1v2)$
1.5163	$8.270\ 832 \times 10^{-4}$	$2.875\ 905 \times 10^{-2}$	$0(0) \rightarrow 1(4v8,3v6,1v4)$
1.5166	$7.056\ 291 \times 10^{-4}$	$2.656\ 368 \times 10^{-2}$	$0(0) \rightarrow 1(3v8,2v6,1v2)$
1.5248	$7.014\ 539 \times 10^{-4}$	$-2.648\ 497 \times 10^{-2}$	$0(0) \rightarrow 1(3v8,4v6,1v4)$
1.5251	$6.327\ 516 \times 10^{-4}$	$-2.515\ 455 \times 10^{-2}$	$0(0) \rightarrow 1(2v8,3v6,1v2)$
1.5711	$5.168\ 603 \times 10^{-4}$	$-2.273\ 456 \times 10^{-2}$	$0(0) \rightarrow 1(2v8,2v6,1v4,1v2)$